Study on Effect of Nanoparticles on Dielectric Properties of Silicone Oil Used in High Voltage Equipment

A Thesis Submitted in Partial Fulfilment for The Degree of Master of Electrical Engineering

By

RANITH SARKAR
EXAMINATION ROLL NO.: M4ELE24008
REGISTRATION NO.: 163485 Of 2022-2023

Under the guidance of

Dr. Arpan Kumar Pradhan

DEPARTMENT OF ELECTRICAL ENGINEERING FACULTY OF ENGINEERING AND TECHNOLOGYJADAVPUR UNIVERSITY
KOLKATA-700032

2024

JADAVPUR UNIVERSITY

KOLKATA- 700032, INDIA

FACULTY OF ENGINEERING AND TECHNOLOGY

CERTIFICATE OF RECOMMENDATION

This is to certify that the thesis entitled "***Study on Effect of Nanoparticles on Dielectric Properties of Silicon Oil Used in High Voltage Equipment***" is being submitted by **RANITH SARKAR** (Registration No. 163485 of 2022- 2023), in partial fulfillment of the requirement for the degree of "Master of Electrical Engineering" from Jadavpur University has been carried out by him under our guidance and supervision. The project, in our opinion, is worthy of its acceptance.

Dr. Arpan Kumar Pradhan
Assistant Professor,
Dept. of Electrical Engineering,
Jadavpur University
Kolkata – 700032

Prof. Biswanath Roy
Head, Dept. of Electrical Engineering
Faculty of Engineering and Technology
Jadavpur University
Kolkata – 700032

Prof. Dipak Laha
Dean,
Faculty of Engineering and Technology
Jadavpur University
Kolkata – 700032

JADAVPUR UNIVERSITY

KOLKATA- 700032

FACULTY OF ENGINEERING AND TECHNOLOGY

CERTIFICATE OF APPROVAL

The foregoing thesis is hereby approved as a credible study of Master of Electrical Engineering and presented in a manner satisfactory to warrant its acceptance as a pre-requisite to the degreefor which it has been submitted. It is understood that by this approval the undersigned do not necessarily endorse or approve any statement made, opinion expressed or conclusion therein but approve this thesis only for the purpose for which it is submitted.

Signature of the Examiner(s)

Signature of supervisor

DECLARATION OF ORIGINALITY AND COMPLIANCEOF ACADEMIC ETHICS

I hereby declare that the thesis contains literature survey and original research work by theundersigned candidate, as part of the Masters of Electrical Engineering studies.

All the information in this document has been obtained and presented in accordance withacademic rules and ethical conduct.

I also declare that, as required by these rules and conduct. I have fully cited and referenced allmaterial and results that are not original to this work.

Name : **RANITH SARKAR**

Class Roll no. : **002210802010**

Exam Roll No. : **M4ELE24008**

Registration no. : **163485 of 2022-2023**

Title of the thesis **:** ***Study on Effect of Nanoparticles on Dielectric Properties of Silicon Oil Used in High Voltage Equipment***

Signature with date:

ACKNOWLEDGEMENT

I express my deep sense of gratitude to my supervisor, **Prof. Arpan Kumar Pradhan,** Department of Electrical Engineering, Jadavpur University for his keen interest, cherished guidance and constant inspiration during the course of the research work. I am obliged and grateful to them for their guidance and giving the opportunity to work in the High Voltage Laboratory. Above all, without their moral support and constant guidance, I would not have completed the work.

I express my sincere gratitude to **Prof. Biswendu Chatterjee, Dr. Sovan Dalai, Prof. Sivaji Chakravorti** and **Prof. Kesab Bhattacharya,** Department of Electrical Engineering, Jadavpur University, for their encouragement, advice and active support in this work. He also worked equally hard to make this work reach its conclusion and beyond. I also convey special thanks to the **High Voltage Laboratory** of Jadavpur University, Kolkata, for providing facility and support during this research work.

I am also thankful to **Dr. Biswanath Roy**, Head of the Department of Electrical Engineering, Jadavpur University, for providing the necessary facilities for carrying out this research work.

I am taking the opportunity to express my humble indebtedness to **Mr. Biswajit Chakraborty, Mr. Sandipan Kumar Paul, Mr. Soumyadeep Maity** research scholar, High Voltage Laboratory, for his invaluable inputs during this work. I am also thankful to rest of the research scholars of High Voltage laboratory for their supportthroughout the tenure of the research work.

I would like to thank my dear friend**s Shahzaib Khurrum** and **Rajdeep Barua**, PG scholars, EE Department, from whom I received immense support, inexplicable encouragements and assistance. I would like to conveymy soulful thankfulness to the rest of the PG scholars of EE. Department for their moral supportduring this course work. I am extremely grateful to my parents and my elder sister for their constant support and motivation, without that I would not have come to this stage. This thesis,a fruit of the combined efforts of my family members, is dedicated to them as a token of love and gratitude.

Above all, it is the wish of the almighty that I have been able to complete this work.

Table of contents

CHAPTER 1

INTRODUCTION

1.1 Introduction and Literature Survey

Silicone oil is a synthetically produced nonpolar dielectric liquid that has applications as an insulating oil in various electrical installations. Its outstanding dielectric qualities include a high flash point, a low loss factor, oxidation resistance, and a high breakdown voltage. However, silicone oil is highly environmentally sensitive due to its extremely low biodegradability. Cable joints are regarded as a beneficial component of distribution networks and the power system. The insulating medium of the cable joints primarily determines their lifespan and state of repair. Because silicone oil has superior dielectric qualities, it can be used to insulate high-voltage equipment like circuit breakers as well as joints. Silicone oil is a synthetic liquid insulation that is very effective, inexpensive, and has a good pouring point and thermal cooling capacity. The need to find a new class of insulation with better dielectric qualities is heightened by the rising power demand of today. To further improve silicone oil's dielectric qualities, the idea of nanotechnology has been used to the insulating base oil in this case. Dr. Choi first proposed the concept of "nanofluid" in 1995. A relatively new byproduct of nanotechnology called nanofluid (NF) is employed as a dielectric and coolant fluid. It is created by evenly dispersing colloidal particles whose diameters are usually between 1 and 100 nm into standard base fluids [5, 6]. Surfactants and dispersants are likely to be included during the manufacture of nanofluids in order to guarantee long-term stability. Because of the enormous surface to volume ratio (S/V) of the nanoparticles, the surfactants are added to the nanofluids to prevent agglomeration. The enhanced surface area, significant heat flow rate, and better breakdown strength are just a few of the many benefits that Dr. Choi [7] found in the nanofluids over traditional liquid dielectrics. Silicone oil is mostly combined with three different types of nanoparticles: conducting, semiconducting, and insulating. The primary criterion used by the researchers to improve the dielectric qualities of insulating oil is an increase in dielectric strength. Insulating nanoparticles are shown to be more appropriate in this situation than conducting and semi-conducting nanoparticles. However, the primary problem that makes using nanofluids for an extended period of time difficult is their instability of dispersion. Optimizing the concentration of nanofluids in base oil is deemed crucial for the manufacture of stable nanofluids over an extended period.

In recent times, silicone oil has been successfully used as an insulation due to its insulating properties. According to [2] moisture in the insulation and excessive temperature rise in the cable mainly responsible for the cable failures. Cables are considered one of the most

important electrical components as it has been potentially able to transmit electricity to the consumers. It has been proven that cables are a valuable component and have an immediate impact on the transmission network. Any disruption related to the cables will decrease the reliability of the power system. As per [2], moisture in the insulation and excessive temperature rise in the cable are mainly responsible for the cable failures. Hence, to overcome cable failure caused by the aforementioned factors, many researches and approaches have been introduced. For this purpose, various nanoparticles mainly (conducting, semiconducting and insulating) have been dispersed in the silicone oil to enhance dielectric characteristics.

Nanofluids are defined as the uniform dispersion of nanoparticles in the base fluid. Due to its exceptional dielectric qualities, it attracted a lot of attention by the researchers [6-7]. In addition, scientists are looking to figure out the ideal ratio of silicone oil (nanofluids) to nanoparticles in order to get better dielectric properties [7]. When a breakdown occurs at a cable termination, huge amount of energy will be extricated from insight of the oil-filled termination. When it explodes, the surrounding equipment sustains harm [3-4]. These damaged terminations are comparable, and there has been a significant amount of harm. It is clear that in cold weather, the silicone oil that was left above the cable's outer semi-conductive layer fractured and solidified, adhering to the main insulation. Silicone oil used in cable terminations has a high pour point, which makes it easy to transition from a liquid to a solid at low temperatures even though it has good thermal stability and water resistance. Consequently, silicone oil has the notion of nanotechnology applied to it in order to improve its dielectric qualities. Now to increase the heat dissipation of insulation oil, Siginer *et al.* first suggested an insulation oil-based nanofluid in 1995 [8]. According to a report in [9], the solidification of coated and filled silicone oil results in varying air gaps. These variations in air gaps cause varying degrees of electric field distortion in the cable termination, particularly at the interface between the cable insulation and stress cone. The insulating property of the contact can be effectively enhanced by coating of silicone oil at room temperature. The asymmetric solidification of silicone oil and the electric field distortion around various sized and positioned air gap flaws within the termination [9]. Although the dispersion of nanoparticles into the silicone oil is advantageous, but due to the large surface to volume ratio (S/V) of nanoparticles, there is a tendency for agglomeration or sedimentation in the nanofluids. As a result, while preparing nanofluids, extra ingredients like surfactants and dispersants are probably going to be needed to assure the long-term stability [10]. According to [11] The best electrical qualities are exhibited by

silicone oil, which also has a reduced moisture content, permittivity, and tan delta losses that are less impacted by moisture intrusion. Silicone oil also has excellent thermal characteristics and is non-hazardous. Therefore, based on the aforesaid observations, it has been clearly indicated that, incorporation of nanoparticles into the base oil has been effectively used to replace the conventional dielectric fluids in the cable joints, while nanofluids can improve thermal and electrical properties, they also need to be resistant to other stressors including electrical and thermal ones. In addition, it is important to conduct routine assessments of the insulation at the cable sealing end in order to prevent premature cable joint failure. The investigation has been conducted in the time and frequency domains. The polarization & depolarization current (PDC) and recovery voltage measurement (RVM) are considered very effective techniques in the time-domain measurement. Whereas, frequency domain spectroscopy (FDS) is a very effective technique in the frequency domain for the determination of the dielectric properties. Therefore, FDS is more beneficial than the time domain [12-14].

In this work, three different nanoparticles (Fe_3O_4, TiO_2, Al_2O_3) were dispersed in the silicone oil that acts as the base oil of the nanofluids with a 1.2% volume fraction to make three different nanofluid samples. Then, PDC and FDS measurements were performed on the produced nanofluids. These measurements were carried out in different temperatures and fixed percentage concentrations of the nanofluids. Hence, from FDS and PDC measurements, some parameters have been extracted through which dielectric properties of the nanofluids can be predicted.

1.2 The Motivation for the Work

With the recent advancement in the field of nanotechnology, nanofluids are widely being preferred in the power system industry due to its large surface area and ability for the enhancement of breakdown strength. Hence, a comprehensive study has been done in this thesis work, for the enhancement of dielectric capabilities of the silicone oil by applying the concept of nanotechnology.

Here in the experiment, condition assessment of the transformer insulation has been carried out through dielectric spectroscopic measurements in both the time and frequency domains. Moreover, from the dielectric spectroscopic measurements, various parameters have been extracted through which dielectric properties of different nanofluid samples can be predicted. Therefore, the aim of this thesis work is to monitor how these parameters of the nanofluids are sensitive to the different temperatures.

1.3 Outline of The Thesis

The structure of the thesis is as follows:

- Chapter 1 introduces the preliminary idea of the thesis work and existing previous works related to this work. It includes my motivation for the work.
- Chapter 2 consists of detailed information regarding cable joints and application of nanotechnology in silicone oil.
- Chapter 3 provides a brief theory about time and frequency domain spectroscopic measurement.
- Chapter 4 consists of the preparation of nanofluid samples involving necessary steps. Further, an experimental set-up was developed to conduct time and frequency domain spectroscopic measurement (FDS, PDC).
- Chapter 5 discusses experimental results obtained from dielectric spectroscopy in the time and frequency domain (FDS, PDC). From these results, a few parameters were extracted from PDC and FDS. Using these parameters, the dielectric performance of the silicone oil has been predicted.
- Chapter 6 discusses the conclusions of this work and states a few challenges that need to be explored in the future.

CHAPTER 2

OVERVIEW OF CABLE JOINTS

2.1 POWER CABLE JOINTS

Cable joints and terminations are essential for cables to provide a stable electrical connection, mechanical support, and physical protection. They are essential components of every home or business' electrical system.

The control and functioning of the power cables play a major role in the reliability of the power transmission system. Power cables are essential for electricity transmission and distribution networks because they carry bulk conductors that transmit power from source to load, facilitating effective energy transfer.

The joints are divided into groups based on the kind of cable, construction material, and function. Cable joints serve as a means of joining cables with different voltages, claims [15]. The structure, insulation, number of cores, and voltage of the cable that needs to be joined determine its shape, size, and configuration. In addition to providing electrical insulation, the joints provide the cables with the necessary strength and mechanical protection. Several electrical connections, such as those formed by soldering, crimping, or utilizing mechanical connectors, are made using the transition junction, branch joint, and PILC joint.

Different cable joints have different mechanical arrangements and different applications for which they are necessary-

I. **Branch Joint**: Branch joints are suitable for outdoor, interior, subterranean, and submerged cable jointing. It is best suited for joining polymeric, low voltage, non-shielded cables ranging from 1 to 5 cores. These can be either 'T' or 'Y' types.

II. **Transition Joint:** Transition joints can be used for any voltage level, cable structure, or insulation type. This junction allows you to safely connect one core cable to a three-core cable. Serving as a crucial medium for bridging traditional paper-insulated cable technology to polymeric cables.

III. **Straight Joints**: This form of junction is excellent for extending cable in any application. They are appropriate for outdoor, interior, subterranean, and submerged cable jointing.

IV. **Pot End Joints**: These sorts of couplings are utilized when electricity wires need to be securely terminated but must be abandoned temporarily or permanently for various reasons.

Insulation materials, such as insulating oils or synthetic materials, are used to avoid electrical breakdown and ensure the safe and reliable operation of the cable. The strength

of the insulation and regular inspection are the two most crucial components that ensure the health of a cable [16]. It has been seen that insulation materials with high dielectric strength can withstanding high voltage without allowing electric current to pass through them. To achieve this, cable joints use insulating oil which offers the necessary thermal stability, electrical insulation, and arc prevention in the event of a fault. Silicone oil is used as liquid insulation in the majority of cable joints due to its extensive dielectric properties and resistance.

2.2 Cable Sealing Ends (CSE)

A cable sealing end is a device or structure that is being used to seal the end part of a cable outer sheath. It is designed to ensure the reliability of the connection and sealing of the cable, allowing it to be used in various environments, including deep-sea applications.

Different sealing structures have been developed to accommodate cables of different diameters and thicknesses, increasing the versatility of the sealing process [25]. These sealing caps or structures typically consist of multiple components, such as sealing cores, sealing pressing sleeves, cylindrical caps, circular table sleeves, and heat-shrinkable tubes. They may also incorporate features like compression springs, adhesive layers, clamp marks, and inflating valve cores to enhance the sealing effectiveness and protection of the cable ends. The manufacturing methods for these sealing caps are designed to be simple and efficient, ensuring a high level of water blocking and durability. In Fig. 1, a typical 132kV cable joint, HV sealing end is shown below.

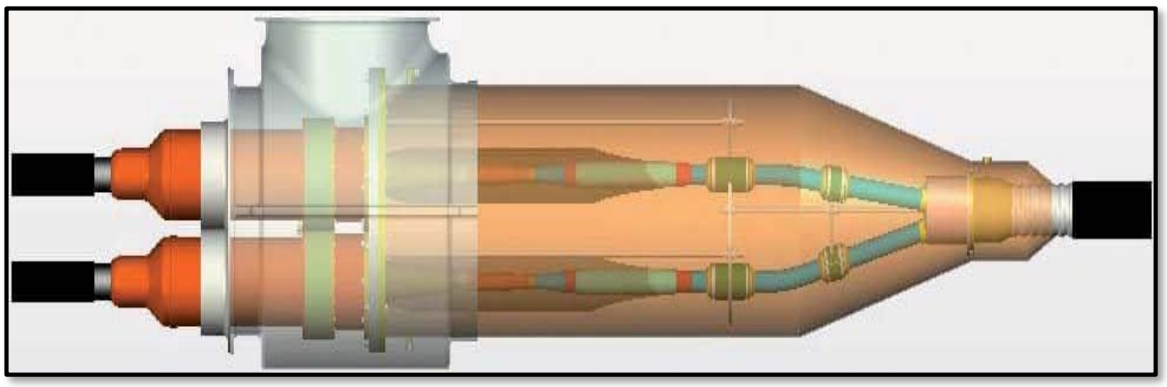

Fig. 1: 132kV Cable Sealing Ends, Terminations & HV Cable Joints

2.3 Silicone oil as Insulation

The existing polymeric cable sealing end (CSE) typically contains silicone oil as an insulating liquid between the cable core and the outside of the CSE. Silicone oil is a synthetic liquid insulation. It has excellent dielectric properties such as breakdown voltage, low loss factor, resistance to oxidation and has a high flash point. However, silicone oil has very low biodegradability which is very vulnerable to the environment, but silicone oil has the highest DC resistance of all insulating oils. According to [24] Synthetic silicone oil (SO) was created in the 1970s to replace askeral oils due to its high flash point and oxygen stability. A recent investigation on silicone oil samples extracted from CSE after decades of use found no significant variation in FT-IR and moisture absorption as compared to the virgin condition. For a CSE, the fundamental priority is to guarantee that the arrangement can operate maintenance-free during the intended lifetime, and the biodegradability of silicone oils and mineral oils is lower than ester oils. that's why silicone oil is most preferable insulation oil among other insulating oils. According to [11] Silicone oil offers the most desirable features, such as reduced moisture saturation, better thermal characteristics, and is non-hazardous. It also has a lower moisture content, permittivity, and tan delta losses, which are least impacted by moisture entry.

For this reason, mostly silicone oil is used as the insulating oil in cable sealing ends. Silicone oils are good insulating liquids across a wide temperature range due to their low glass transition values, and they have the potential to be used not just offshore but even in extraterrestrial applications.

2.4 Study of Nano fluids

It has been reported in [16], Feynman introduced the idea of nanotechnology in 1959. That has been used in several scientific disciplines, most notably physics, engineering, material science, etc. Using nanotechnology, it becomes possible to manipulate the matter at the nanoscale (roughly in the range of 1-100 nm) which efficiently improves the materials' various characteristics. The same idea holds true for nanofluids, which are dielectric liquids that possess nanoparticles incorporated to improve their thermal and dielectric properties. The term "nanofluid" was first introduced by Dr. Choi and Eastman in 1995. The nanofluids are the base fluids that have nanoscale particles uniformly floating throughout them. As per [26,27], In accordance to many researchers, adding nanoparticles into transformer oil will raise the breakdown voltage. Researchers are still looking for a perfect combination of nanoparticles and transformer oil (nanofluids) to have superior

characteristics. In addition to having significant effects on the thermal properties of composite materials, the volume percentage of nanoparticles, surface to volume ratio (S/V), shape and size, and surface region of contact between particles and liquid are critical standards.

2.4.1 Types of Nanoparticles

Nanoparticles can be roughly categorized into a number of groups based on their morphology, size, and chemical characteristics. The choice of nanoparticles for the fabrication of nanofluids must be made with extreme care. Typically, permittivity and conductivity are used as the primary criterion for selection. Therefore, First, analyze all of the material's qualities, which will help in improving the fluid's dielectric strength. Nanoparticles are roughly classified into three primary categories-

- **Insulating nanoparticles**
  Some well-known insulating nanoparticles are boron nitride (BN), Alumina (Al_2O_3) and silicon oxide (SiO_2)
- **Conductive nanoparticles**
  Ferrous ferric oxide (Fe_3O_4) and zinc oxide (ZnO) these nanoparticles are conductive in nature.
- **Semi-conductive nanoparticles**
  Examples of semi-conductive nanoparticles are titanium dioxide (TiO_2), copper oxide (CuO_2).

2.4.2 Dielectric properties of nanoparticles

The dielectric characteristics of nanofluids will unavoidably alter significantly as a result of the addition of nanoparticles [17-18]. According to [19] The results show that introducing nanoparticles significantly raised the electrical resistivity, the imaginary component of the dielectric constant, and the dielectric loss factor, but the relative permittivity remained constant until the volume fraction of nanoparticles reached 0.016. Nanofluids have a dielectric loss value of 0.1868, which is 51 times greater than that of pure oil (0.0036). when the volume percentage of Fe_3O_4 is 0.8%. Additionally, magnetic nanoparticles decrease volume resistivity, making them potentially harmful when used in the electrical field for applications involving nanofluids. Merges *et. al*. investigated the effect of frequency on the dielectric properties of nanofluids, and they reported that in the

frequency range of 10^{-1} Hz to 10^{6} Hz, Fe_3O_4 Based nanofluids had greater relative permittivity, dielectric loss factor is also increased [20]. Du *et. al*. looked at how temperature affected the dielectric characteristics of nanofluids. In various oil temperature ranges, conductive Fe_3O_4 nanoparticles have reduced electrical resistivity and raised the dissipation factor. However, insulated BN nanoparticles had a good dielectric characteristic that enhanced electrical resistance and decreased dissipation factor [21]. Li *et. al.* looked into the dielectric characteristics of a Fe_3O_4 nanofluid made from vegetable oil [17, 22]. When the frequency is below 10 Hz, they observed that the dielectric loss factor of nanofluids is much lower than that of pure oil, however when the frequency is greater than 100 Hz, they observed that the volume resistivity of nanofluids is much greater than pure vegetable oil.

The majority of studies were AC BDV-centric, and there haven't been many investigations into DC BDV or positive impulse voltage. The mineral oil-based nanofluid a Fe_3O_4 (diameter of a Fe_3O_4 nanoparticle is around 10 nm; practically spherical) is at the top of the list with the greatest enhancement in AC and DC BDV and positive impulse voltage. The positive impulse BDV and conductivity of nanofluids that contained rod-like nanoparticles made from TiO2 increased 23 and 60.7%, respectively, as compared to TiO2 nanospheres, according to Lv *et. al.* study of the morphology, which includes the size and shape of nanoparticles that affects their dielectric properties [23].

2.4.3 Advantages and disadvantages of nanofluids

From the aforementioned sections, it can be concluded that the addition of nanoparticles in the base fluids can effectively increases some properties. The nanofluids includes the following advantages,

- The dispersed nanoparticles enhance the fluid's effective thermal conductivity.
- The enhanced specific surface area of the particles increases the interaction between the base fluid and the nanoparticles.

But, due to the large surface area of the nanoparticles, there is a tendency for agglomeration or sedimentation of the particles in the base fluids. Apart from this, the processing expenses of the nanofluids are very high. Also, rapid clustering is a big issue when dealing with the nanofluids.

CHAPTER 3

DIELECTRIC RESPONSE METHOD

3.1 Dielectric Response Method

To prevent cable failure, insulation should be monitored at a time interval before. For this purpose, dielectric response analysis has been employed to evaluate the insulation state of insulating oil. The two basic categories of this investigation are conducted in the time and frequency domain. For these purposes, polarization & depolarization current (PDC) is an effective technique that is used in time-domain spectroscopy measurement. Whereas, frequency domain spectroscopy (FDS) is effectively used in the frequency domain for the determination of insulation capabilities. Hence, a brief theory related to PDC and FDS has been discussed in the following section.

3.1.1 Background of Time Domain Spectroscopy

3.1.2 Polarization Depolarization Current (PDC)

When an electric field is applied to a dielectric, the polarization process begins. The inner dipoles are directed in the direction of the applied electric field as a result of the polarization process. The effects of polarization resulting the displacement current and conduction current to increase. [18,19]. Hence, electric displacement can be defined as,

$$D(t) = \varepsilon_0 \varepsilon_r E(t) + \Delta P(t) \tag{3.1}$$

In this case, the permittivity in free space, relative permittivity of the dielectric material, applied electric field and the polarization function are denoted as $\varepsilon_0, \varepsilon_r$, E(t) and P(t), respectively. P(t) is the dielectric response function that has monotonically decaying characteristics can be written as (3.2).

$$P(t) = \varepsilon_0(\varepsilon_\infty - 1)E(t) + \varepsilon_0 \int_0^t f(t-\tau)E(\tau)d\tau \tag{3.2}$$

ε_∞ is the relative permittivity of the material at high frequencies In (3.2), the first term represents rapid polarization, and the second term represents slow polarization. The current density through a dielectric medium in an electric field may be determined using Ampere's law. E(t). Therefore,

$$J(t) = \sigma E + \varepsilon_0 \frac{\partial}{\partial t}\{\varepsilon_\infty E(t) + \int_0^t f(t-\tau)E(\tau)d\tau\} \tag{3.3}$$

In (3.3), the first term represents the conduction current, and the second term represents the polarization current. The current passing through the test object can therefore be expressed as follows, assuming that external voltage U(t) generates the electric field E(t). Hence the current, due to the effect of DC conductivity, permittivity and dielectric response function can be written as (3.4).

$$I(t) = C_0 \left(\frac{\varepsilon_0}{\sigma_0} + \varepsilon_\infty \delta(t) + f(t)\right) U(t) \tag{3.4}$$

Where C_0 is referred as the geometrical capacitance of the test sample.

Polarization and depolarization current methods are the fundamental elements of time domain dielectric diagnostics. This approach records the insulation's charging and discharging currents. In the time domain, one method for investigating slow polarization processes is to measure polarization and depolarization currents (PDC) after a dc voltage step. The test object's dielectric memory must be cleaned prior to PDC measurement. In order to precisely record the small polarization current, the voltage source has to be free from ripple and noise. The schematic of the PDC measurement has been given in the Fig. 2.

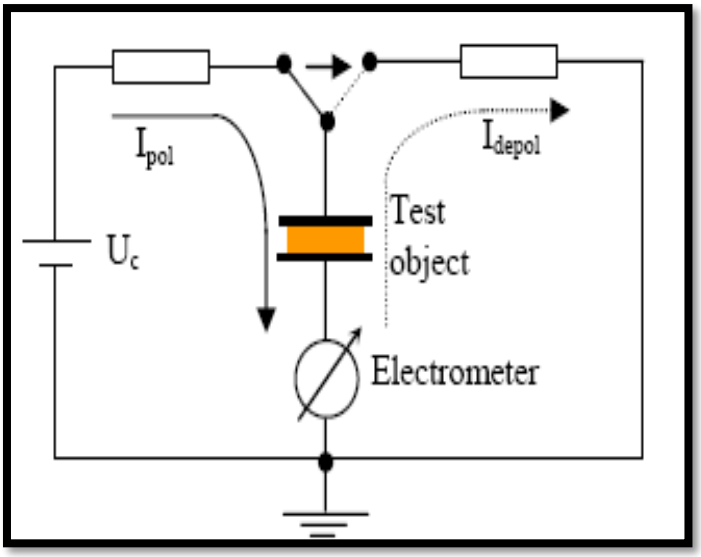

Fig. 2: PDC Measuring Circuit [27]

The test object is subjected to a dc charging voltage with magnitude (U_c) applied over an extended period of time (for example 10,000 sec). During this time, the polarization current $I_{pol}(t)$ through the test object is measured, caused by the activation of the polarization process with varied time constants correlating to various insulating materials and the conductivity of the object, which has

previously been completely discharged. In the following section, typical characteristics of the polarization and depolarization current have been shown in Fig. 3.

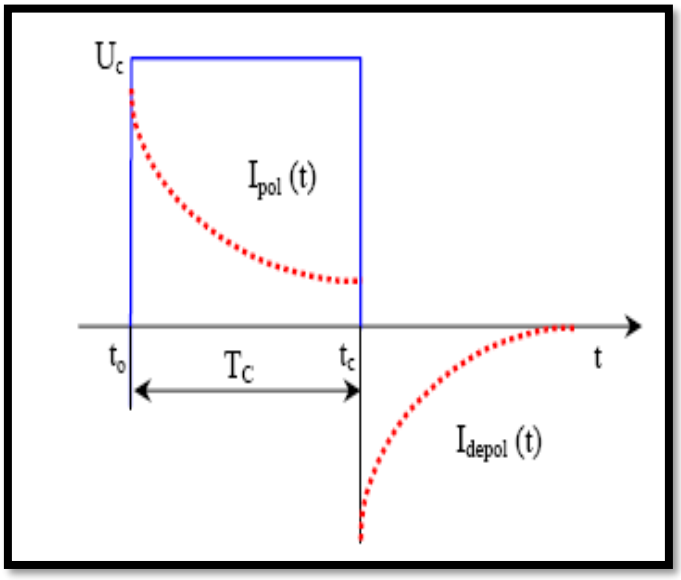

Fig. 3: Typical Nature of Polarization and Depolarization Current [27]

The figure 3.2 illustrates the standard nature of polarization and depolarization current. The DC step voltage Uc charges the insulation between the windings. From Fig.3.2, it has been concluded that, the initial time dependence of the polarization and depolarization currents (<100 s) is very sensitive to the conductivity of the silicone oil. As shown in Fig.3.2, the initial time dependability of the polarization and depolarization currents (<100 s) is very sensitive to the conductivity of the silicone oil.

Therefore, the DC conductivity σ_0 can be expressed by (3.5)-

$$\sigma_0 = \frac{\varepsilon_0}{C_0 V_{dc}} [i_{pol}(t) - i_{depol}(t)] \tag{3.5}$$

3.1.3 RVM

According to the basic idea of recovery voltage measurement, the charging (polarization) and discharging (depolarization) processes may be done using the same circuit as illustrated in Fig.3.1. The discharging time is much less than the charging time, depending on the requirements. Typically, draining time ($t_{discharge}$) is equal to half of the charging time ($t_{charging}/2$). To measure voltage, the electrometer should switch between ammeter and voltmeter modes at the ideal moment. Modern

electrometers may be configured using a computer to change time sequences, making this a non-issue.

Fig. 4, illustrates a typical recovery voltage waveform. The peak value $V_{recovery}$ (peak) and the initial slope are two essential features of the recovery voltage waveform.

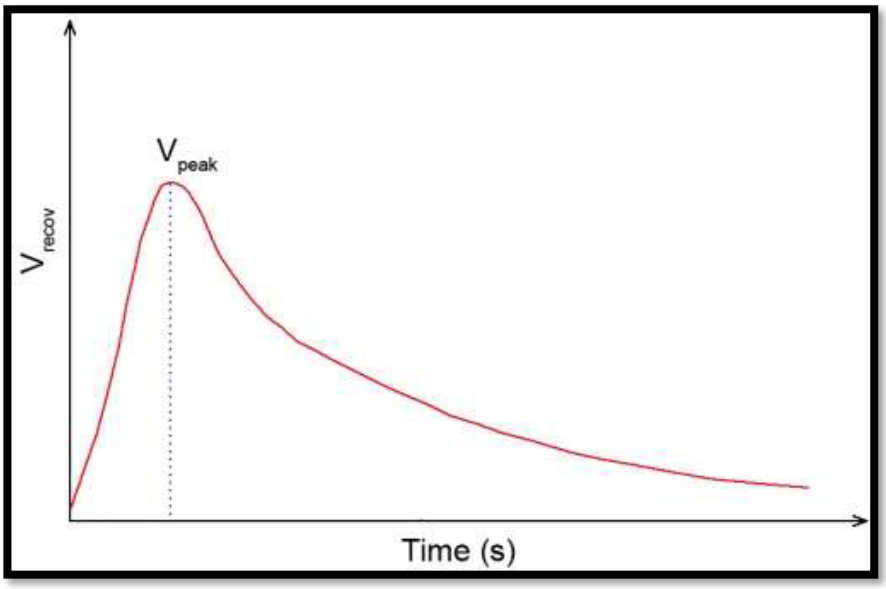

Fig. 4: A Typical Recovery Voltage waveform [26]

3.1.3.1 The central time constant Concept of RV spectra

According to the RV evaluating methodology, described in Section 1.3.2, the charging time gradually increases with the corresponding increase in discharging time from a small starting value, and each step yields a distinct peak value of recovery voltage, $V_{recovery}$ (peak). Peak values obtained for various charging times (t_{ch}) may be plotted to produce a $V_{recovery}$ (peak) vs. $t_{charging}$ curve, known as the recovery voltage spectrum. The recovery voltage spectrum is also examined for condition monitoring. The charging time that corresponds to the peak of the RV spectrum is known as the central time constant (CTC). A representative diagram of recovery voltage spectrum shown in Fig. 5.

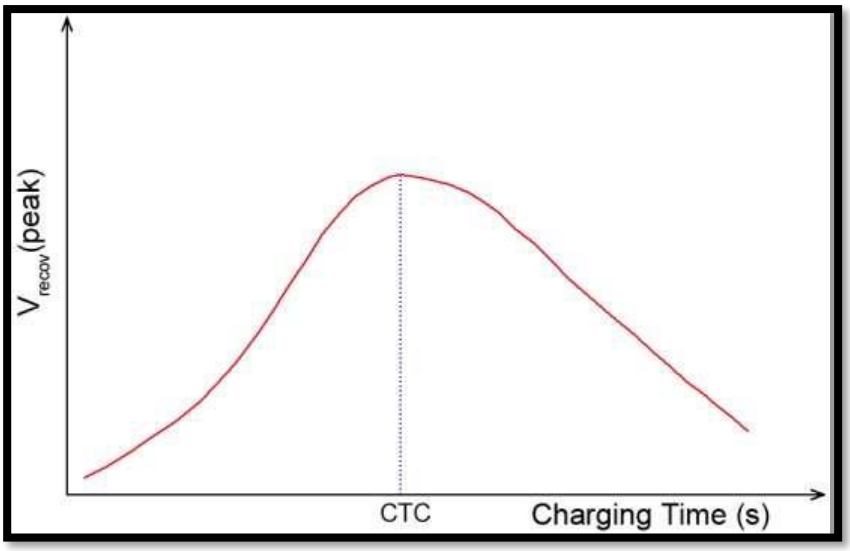

Fig. 5: A Representative Recovery Voltage Spectrum [26]

3.1.4 Estimation of Activation Energy

The activation energy of a dielectric sample gives a brief idea of the barrier potential of the trapped charges that needed to be overcome for conduction in the dielectric material. As mobility of charge carriers depends upon temperature effectively, it has a dominating role on polarization process in dielectric medium as discussed earlier [34]. It can be revealed that the change of conductivity with the change in temperature is associated with the activation energy (E_g). This can be represented by the equation –

$$\sigma = Ae^{\left[\frac{-Eg}{kT}\right]} \tag{3.6}$$

In this equation A, has been a constant, 'k' represents the Boltzmann constant, whose value has been $1.38064852 \times 10^{-23}$ m^2 kg s^{-2} K^{-1}. The activation energy has been graphically figured out using the Arrhenius equation for all the samples.

$$ln(\sigma) = ln(A) - \frac{Eg}{kT} \tag{3.7}$$

It is quite clear that this equation has resembled the equation of a straight line, i.e.,

$$y = mx + c \tag{3.8}$$

From Table 1 the conductivity data obtained at six different temperatures (30°C,40°C, 50°C, 60°C, 70°C, and 80°C) is used to plot a graph of the logarithm of conductivity against the inverse of the absolute temperature. The MATLAB curve-fitting technique has been applied to the obtained curve and calculating the

slope of the obtained curve by comparing it with the equation (3.8). The value of activation energy has been determined by multiplying the slope of the curve-fitted equation by the value of the Boltzmann constant, 'k', mentioned in the equation:

$$Eg = k \times slope \tag{3.9}$$

Using equation (3.9), the activation energy values are calculated in joules (J). The activation energy for each sample is shown in Table 2. These values are then converted to electron-volts (eV) using the conversion factor

$$1eV = 1.6 \times 10^{-19}\, Joules \tag{3.10}$$

3.2 Background of Frequency Domain Spectroscopy

Another approach to studying polarization processes is to investigate dielectric response in the frequency domain. This is an AC test, and the dissipation factor, often known as tan delta, is realized as a function of test frequency. The frequency range for FDS is typically 1 mHz to 40 kHz. This includes measuring impedance at various frequencies and voltages. The dielectric is charged with sinusoidal voltages, and the current across it is monitored. Frequency domain measurements require voltage sources with changing frequencies and, for applications linked to HV power equipment, output voltages of at least a few hundreds of volts. The impedance is then calculated, which aids in the determination of power factor, capacitance, dissipation factor, permittivity, and different variables. In this part the Fig.6, illustrates the basic FDS measuring circuit.

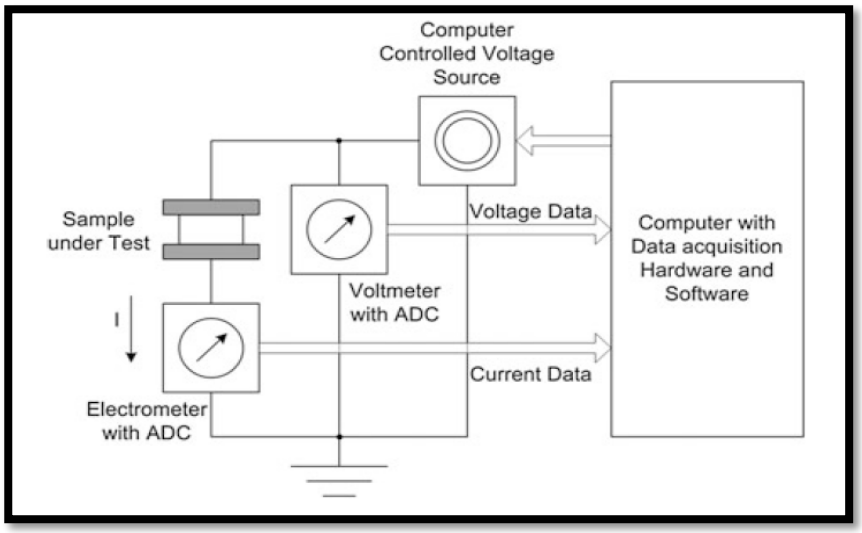

Fig. 6: FDS Measurement Circuit [14]

When an alternating field is established, the dipoles present in the dielectric material continue to align with the electric field. The free electrons present in the insulating material start to travel in the same direction as the anode. The alignment of the dipoles and the flow of electrons toward the anode impact the electric current that travels from the anode to the cathode through the dielectric material. The effect of electron mobility and dipole alignment on each other determines the type of the current. According to [14], the current's quality appears to degrade with time. As a result, the time domain current may be analytically transformed to the frequency domain using the Laplace or Fourier transforms.

Therefore, with the application of pure sinusoidal stimulation, the current flowing through the dielectric material can be determined in the frequency domain as,

$$\overline{I(\omega)} = j\omega\, \overline{C(\omega)}\overline{U(\omega)} \tag{3.12}$$

Where current through the dielectric material is represented by $\overline{I_\omega}$ and the equivalent complex capacitance of the dielectric material is resented by $\overline{C(\omega)}$ .The expression of $\overline{C(\omega)}$ is given in (3.12).

Where $\overline{C(\omega)}$ and $\overline{U(\omega)}$ are the equivalent complex capacitance of the dielectric and applied voltage of frequency (ω), respectively, Again, $\overline{C(\omega)}$ can be further realized as the following equation:

$$\overline{C(\omega)} = C'(\omega) - jC''(\omega) = C_0[\varepsilon'(\omega) - j\varepsilon''(\omega)] \tag{3.13}$$

In (3.13), $\mathcal{E}'(\omega)$ is the real component of the complex permittivity, which in general denotes the capacity to store energy due to dipoles and electrons. Whereas, $\mathcal{E}''(\omega)$ is the imaginary component of complex permittivity, which often represents energy loss during dipole alignment and electron transport. The dipoles interact with the molecules or other existing dipoles when alignment takes place in a dielectric medium under an alternating field. The frictional loss produced by these contacts raises a dielectric loss [15]. The electron is driven towards the anode when an electric field is introduced. As a result, any molecules, electrons, or dipoles that are already present are hit by traveling electrons. By generating energy loss within the dielectric material, this collision increases the dielectric loss. Generally, the imaginary component of the complex permittivity, $\mathcal{E}''(\omega)$ indicated this dielectric loss. In (3.14), $\mathcal{E}'(\omega)$ represents the energy storage capability that takes place in the dielectric material as a result of the electrons'

transporting to the anode and the dipoles' alignment with the applied field. The *tanδ* is a parameter that can be used to estimate the state of an insulating material [16]. It is the ratio between the imaginary component of the complex permittivity, which indicates energy loss, and the energy storage component, or the real part of the complex permittivity, is known as the *tanδ*. The expression of *tanδ* is given as (3.14).

$$tan\delta = \frac{\varepsilon''(\omega)}{\varepsilon'(\omega)} \tag{3.14}$$

According to [14], electron transport in an insulating material under an electric field and the alignment of the dipoles are extremely slow processes that are effective in the power frequency range (i.e. 50 Hz) and below it. To acquire a clear image, frequency domain spectroscopy (FDS) is used at very low frequency ranges, from 1 mHz to 1 kHz or more [8, 10].

3.2.1 Concept of Electric Modulus

By applying an alternating electric field with angular frequency (ω) across an insulator, when the frequency of the electric field is low then accumulation of electric charge takes place near the electrodes. This is called as electrode polarization, which introduces large permittivity as well as bulk dielectric relaxation process in the dielectric material. For this reason, it is difficult to investigate its behaviour. In this situation, complex electric modulus can be view as a very useful tool for analyzing the relaxation behaviour of dielectric material. The inverse of complex electric permittivity($\varepsilon^*(\omega)$) is used to represent the complex electric modulus ($M^*(\omega)$), where the impact of the conductance is ignored.

As a function of frequency, the complex permittivity may be written as (3.15)

$$\varepsilon^*(\omega) = \varepsilon'(\omega) - j\varepsilon''(\omega) \tag{3.15}$$

where the imaginary part ($\varepsilon''(\omega)$) indicates the losses (which includes polarization and conduction losses) that created inside the insulating medium and the real part indicates the energy storage component. The complex electric modulus ($M^*(\omega)$) can be expressed in terms of real and imaginary part of complex capacitance as [29].

$$M^*(\omega) = M'(\omega) + jM''(\omega) \tag{3.16}$$

$$M^*(\omega) = \frac{1}{\varepsilon^*(\omega)} = \frac{1}{\varepsilon'(\omega) - j\varepsilon''(\omega)} \tag{3.17}$$

$$M^*(\omega) = \frac{\varepsilon'}{\varepsilon'^2 + \varepsilon''^2} + j\frac{\varepsilon''}{\varepsilon'^2 + \varepsilon''^2} \tag{3.18}$$

$$M"(\omega) = \frac{\varepsilon"}{\varepsilon'^2+\varepsilon"^2} \tag{3.19}$$

$$M'(\omega) = \frac{\varepsilon'}{\varepsilon'^2+\varepsilon"^2} \tag{3.20}$$

Here from (3.18) $M'(\omega)$ indicates the real part and $M''(\omega)$ indicates the imaginary part of complex electric modulus $M^*(\omega)$ respectively. From (3.17) if, at low frequency due to electrode polarization the values of $\varepsilon'(\omega)$ and $\varepsilon"(\omega)$ becomes very high then $M'(\omega)$ and $M''(\omega)$ becomes small. As $\varepsilon'(\omega)$ and $\varepsilon"(\omega)$ are appeared in the dinominator. As a result, the huge permittivity value generated by electrode polarization in the permittivity spectrum does not show up in the electric modulus spectrum, supressing the relaxation process. So, from (3.16) the relaxation moves to higher frequency in the electric modulus spectrum analogous to permittivity spectrum. Thus, analysis of the electric modulus spectrum may provide an additional data than the permittivity spectrum on the relaxation behaviour of insulating oil.

CHAPTER 4

EXPERIMENTAL SETUP

4.1 Preparation of test sample

For investigation of the insulation properties of silicone oil based nanofluids, an experimental set-up was developed in the laboratory. For this purpose, silicone oil (SO) was selected as the base oil and three different nanoparticles have been selected to prepare nanofluid samples. In the selection of the nanoparticles, conductivity and permittivity are the two primary parameters that must be considered. Here three different nanoparticles have been considered-

- Alumina (Al_2O_3), insulating nanoparticle
- Ferrous ferric oxide (Fe_3O_4), conducting nanoparticle
- Titanium dioxide (TiO_2), semi-conducting nanoparticle

The entire process is classified into six steps, as follows:

i. At first, selected nanoparticles i.e. Fe_3O_4, TiO_2 and Al_2O_3 were measured individually on a high precision weighing Scale. Then 0.048 mg of each nanoparticle were transferred in a plastic cup and 2 ml of oleic acid (cis-9-Octadecenoic acid) was added to each nanoparticle. Mixing the nanoparticles with surfactant was carried out by a magnetic stirrer for around 30 minutes with 900 rpm-1000 rpm.

ii. In four identical beakers, 400 ml of silicone oil was taken into each beaker and heated for two hours at 80℃. Then the solution of nanoparticle and surfactant were dispersed in the heated silicone oil solution to get a concentration of 0.12gm/l.

iii. To ensure homogeneous agglomeration-free dispersion of the nanoparticles, all the prepared nanofluid solutions were applied to ultrasonication for 99 minutes successively.

iv. After the sonication procedure, prepared nanofluid samples were carried out in a degassing chamber for at least an hour.

v. Four electrodes were made up of two 14.00 cm × 4.00 cm aluminium sheets spaced apart by 4 mm each. The structure of the electrode is shown in Fig. 7. After that, the electrode is dipped into the prepared nanofluid sample and necessary precautions are taken of.

vi. Aluminium foil has been used to secure the top of the beakers to protect the prepared nanofluid samples from any kind of dust.

Here, in Fig. 8, block diagram of the entire preparation procedure of the nanofluids was shown. Both time and frequency domain spectroscopy measurements have been conducted on silicone oil based nanofluid samples.

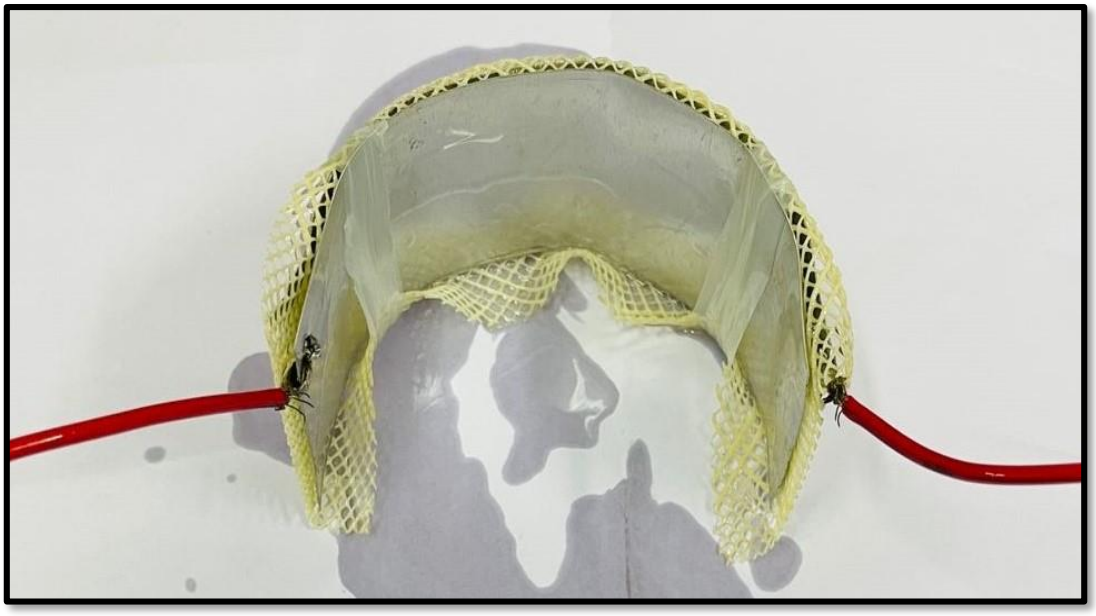

Fig. 7: Electrode set-up

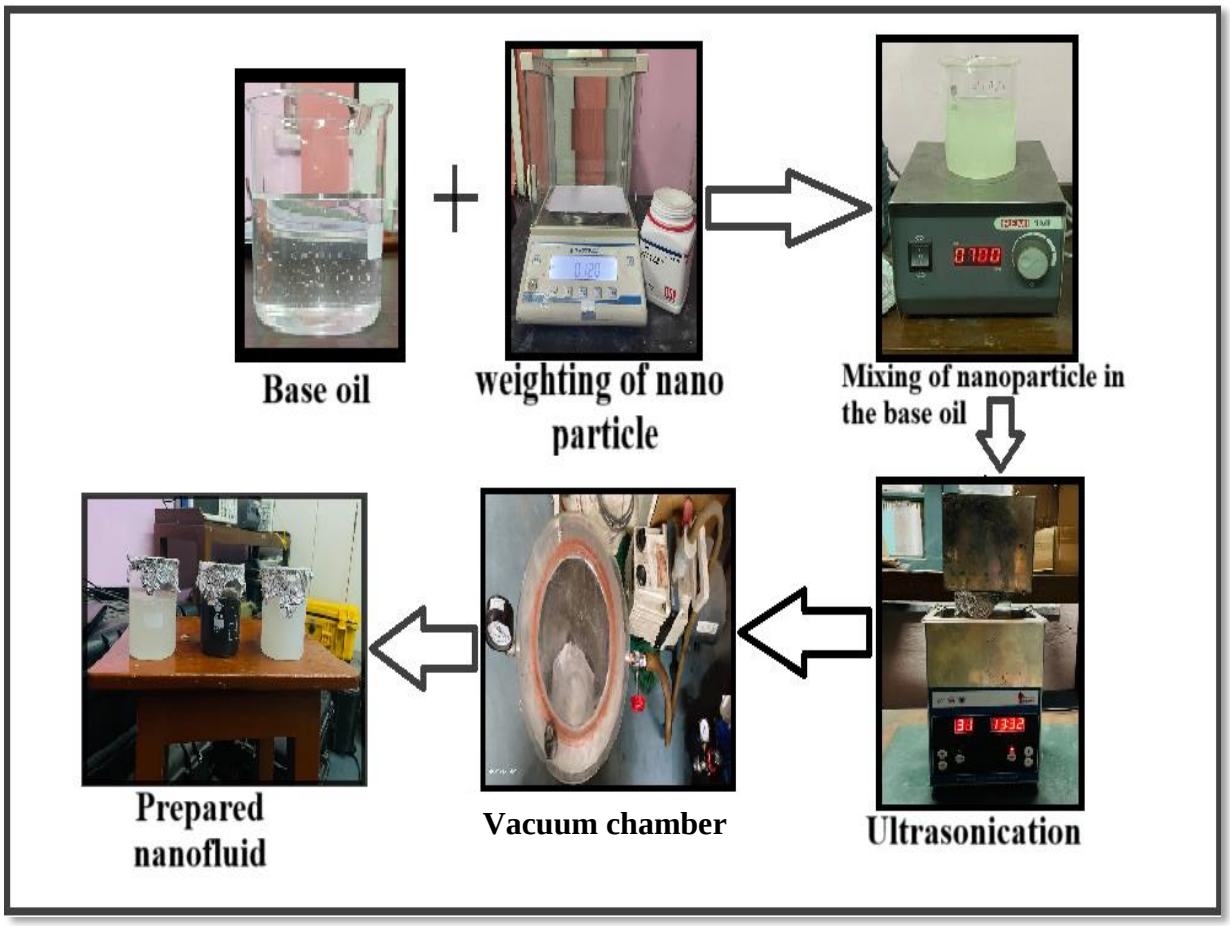

Fig. 8: The procedures needed to prepare silicone oil based nanofluid samples

4.2 Setup and Procedures

In this section, experimental procedures for investigation of the insulating properties of nanofluid samples have been discussed in both time and frequency domains. In this context, Fig. 9 and Fig. 10, describes the experimental setup used for PDC and FDS measurements.

4.2.1 Time Domain Spectroscopy on Prepared Sample

For investigation of the insulation capability of laboratory prepared silicone oil based nanofluid samples, time domain spectroscopy has been conducted employing DIRANA^{TM} at different temperatures 30°C, 40^{0}C, 50^{0}C, 60^{0}C, 70^{0}C, 80^{0}C and source voltage is 200V.

For time domain spectroscopy measurement, at first, every nanofluid samples along the pristine silicone oil sample was heated to the desired temperature for 4 hours each then polarization and depolarization currents were recorded for 1000 seconds of each sample. Fig.9. describes the experimental setup of PDC measurement.

Fig. 9: Experimental Setup for PDC Measurement

4.2.2 Frequency Domain Spectroscopy on Prepared Sample

The insulation characteristics of laboratory-prepared silicone oil-based nanofluid samples have been investigated employing frequency domain spectroscopy (FDS) measurement performed using an insulation diagnostic analyzer (IDAX 300 by Megger) at

various temperatures. In this study, the voltage magnitude of the FDS measurement was set to 140 V_{rms}. At first, every nanofluid samples along pristine silicone oil sample was heated to the desired temperature for 4 hours each. FDS measurement was recorded for a wide range of frequencies (1mHz to 40kHz). Fig 4.4 describes the experimental setup of FDS measurement.

Fig. 10: Experimental Setup for FDS Measurement

4.2.3 AC Breakdown Voltage Measurement

AC breakdown voltage is defined by the value of applied AC voltage at which disruptive discharge is initiated in the liquid. Therefore, the measured AC breakdown voltage of an insulating liquid mainly indicates the oil quality rather than the properties of oil itself. As instructed in IS 6792:1992 to evaluate the ac BDV, an appropriate quantity of insulating oil is placed within a test shell where two electrodes (with a diameter of 12.5 mm) have been separated by 2.5 mm [1].

The breakdown voltage of the laboratory-prepared silicone oil-based nanofluid samples were measured by implementing the Breakdown Test kit by NTPL. At first, every nanofluid samples along pristine silicone oil sample have been heated at 60^0C for 2 hours each followed by a degassing session of 1 hour, Then the BDV of the test samples was measured in the test kit. The rate of voltage rise was 2 kV/s in this test setup. The BDV of the test samples has been conducted six times, the time break between two consecutive dielectric breakdown tests on the same sample was around 5 min and the average value was

considered. Fig. 11, describes the experimental setup of AC breakdown voltage measurement.

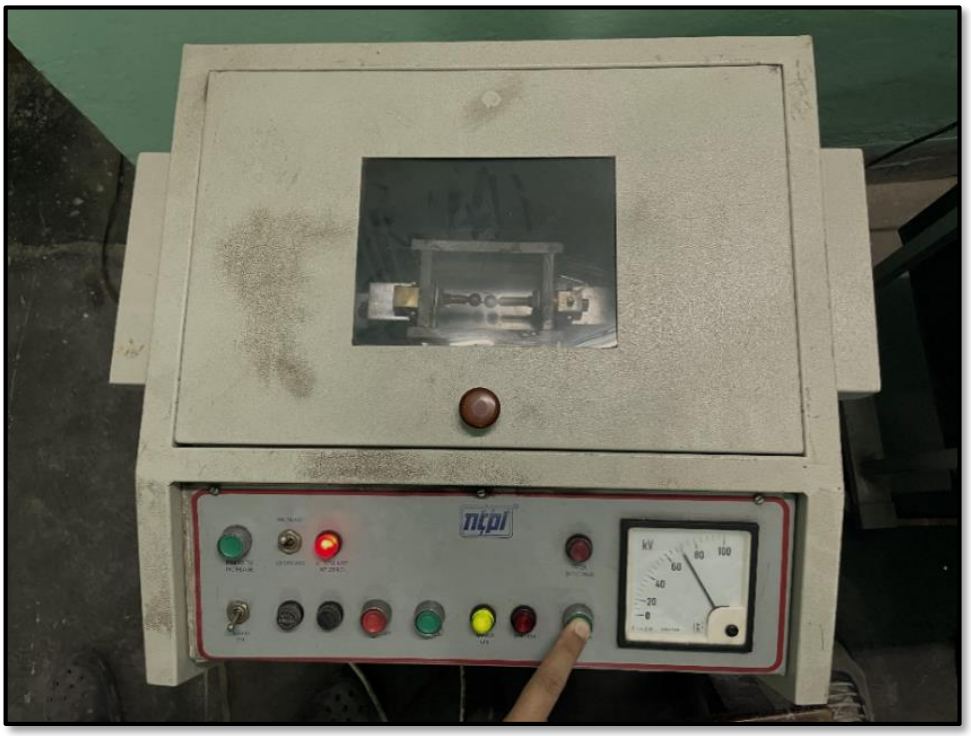

Fig. 11: AC Breakdown Voltage Measurement Kit

CHAPTER 5

RESULTS AND DISCUSSIONS

5.1 Analysis of the results obtained from PDC

In this section, dielectric response measurements in the time domain have been discussed. At first, the influence of nanoparticles on the polarization and depolarization current (PDC) characteristics of silicone oil based nanofluids has been discussed. In addition, a comparative analysis of PDC curves obtained from pristine along with three nanofluid samples has been performed to investigate nanofiller induced modification in dielectric properties

5.1.1 Variation of polarization currents with temperature

In this section the effect of temperature on the polarization current of the dielectric insulation have been studied. In Fig. 12, the polarization current of pristine silicone oil has been plotted for 30^0C, 40^0C, 50^0C, 60^0C, 70^0C and 80^0C respectively. It can be concluded from the curve, that the polarization current is increased along with the temperature rise. This phenomenon can be described due to a fact that, for higher thermal energy number of free electrons are increased.

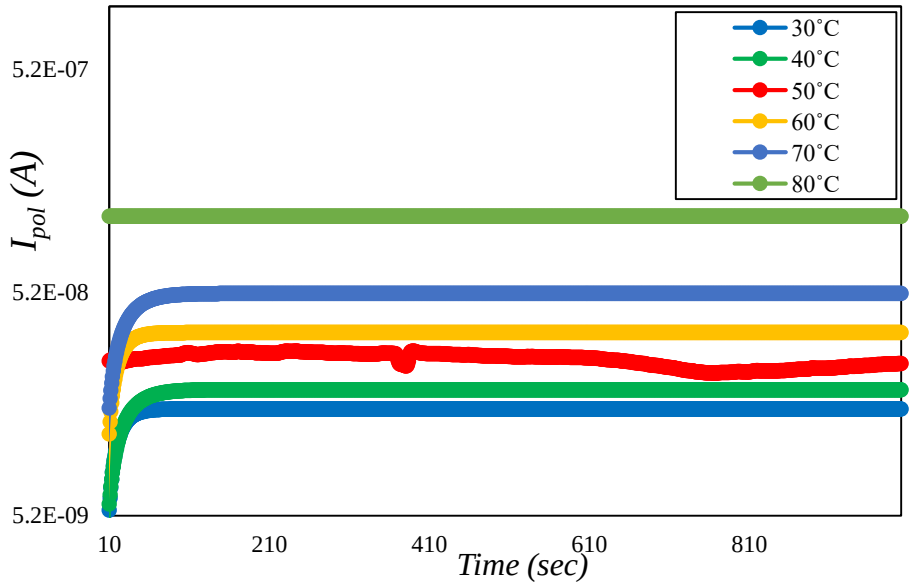

Fig. 12: Polarization currents of pristine silicone oil at different temperatures

From the Fig. 12, it can also be observed that, the increment rate of the polarization current of pristine silicone oil is higher for higher temperatures like 70^0C and 80^0C than the increment rate of polarization current of lower temperatures like 30^0C, 40^0C, 50^0C. so, it can be concluded that, pristine silicone oil showed better insulation properties in lower temperatures.

5.1.2 Variation of polarization currents with different nanoparticles

In this section the effect of different nanoparticles on the polarization current of different prepared silicone oil based samples have been studied at different temperatures. In Fig. 13 - Fig. 14, the polarization current of different prepared silicone oil-based samples has been plotted for 30^0C and 80^0C respectively. It can be observed from Fig. 13 - Fig. 14 that, irrespective of temperatures, silicone oil based nanofluids have shown considerably lower polarization current than pristine silicone oil. This phenomenon occurred due to the incorporation of nanoparticles into the dielectric medium. The interfacial region has been modified, by which NP can restrict charge migration in the interfacial region of the insulation. This in turn reduces polarization, as a result of which $I_{pol}\,(t)$ of nanofluids has been observed to be significantly lower. Si-oil+TiO_2 sample has shown least polarization current among all. Therefore, it can be dictated that presence of TiO_2 NP leads to the formation of strong bonds between adjacent polymer chains. As a result, the mean free path for mobile charge carriers reduces, which restricts the space charge migration. This fact causes DC conduction current to reduce substantially even at a high temperature such as 80^0C. In view of this, Si-oil+TiO_2 can be considered as the most suitable nanofluid in showing imperative dielectric property under extreme thermal stress. Fig. 13 Variation of Polarization current of different samples at 30^0C.

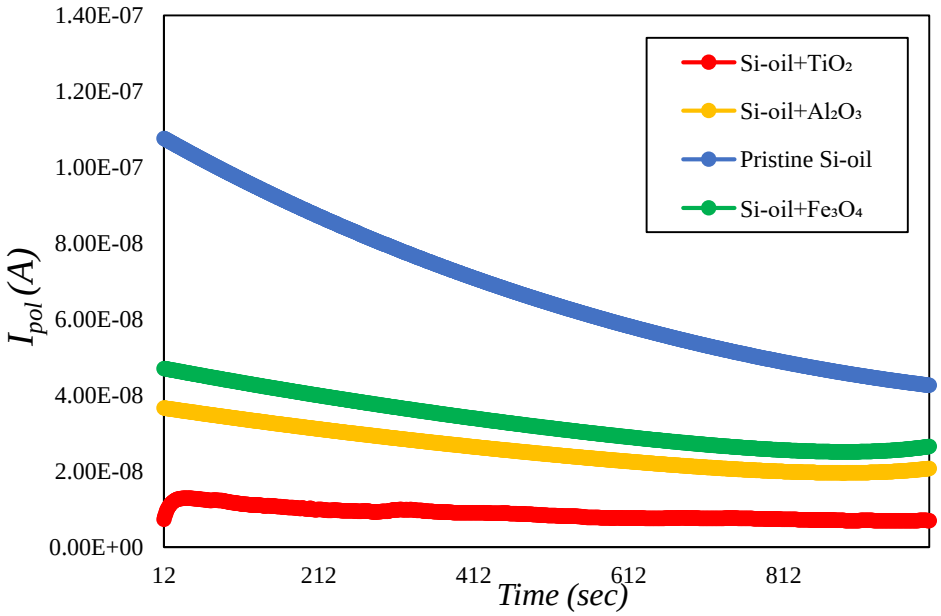

Fig. 13: Variation of Polarization current of different samples at 30^0C

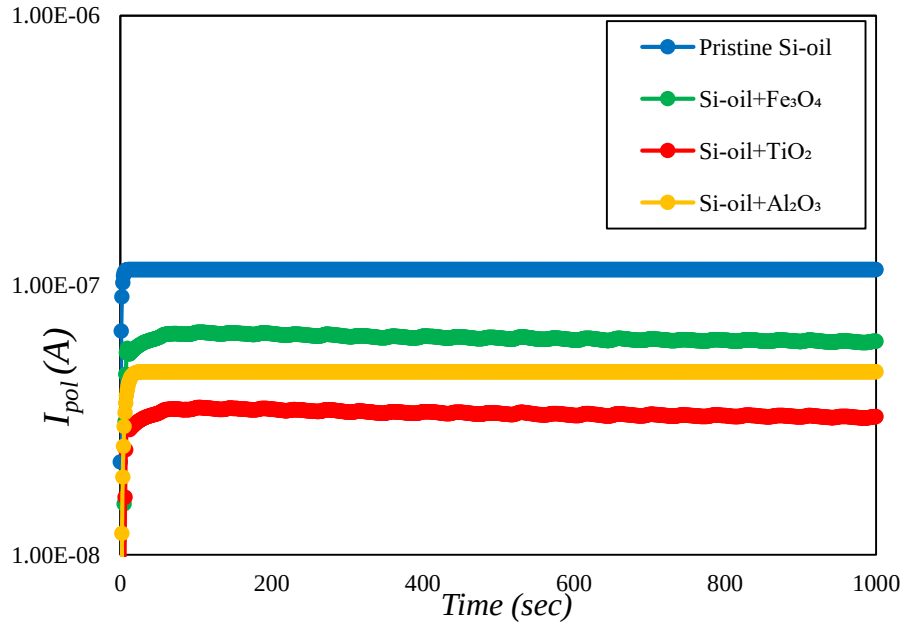

Fig. 14: Variation of Polarization current of different samples at 80^{0}C

5.1.3 Variation of depolarization current with different nanoparticles

In this section the effect of different nanoparticles on the depolarization current of different prepared silicone oil based samples have been studied at different temperatures. In Fig. 15 - Fig. 16, the polarization current of different prepared silicone oil based samples has been plotted for 30^{0}C and 80^{0}C respectively. It can be observed that nanofluids samples have shown considerably lower depolarization current than pristine silicone oil irrespective of temperatures change. Hence, it can be concluded that the incorporation of nanoparticles has caused a significant improvement by supressing depolarization current.

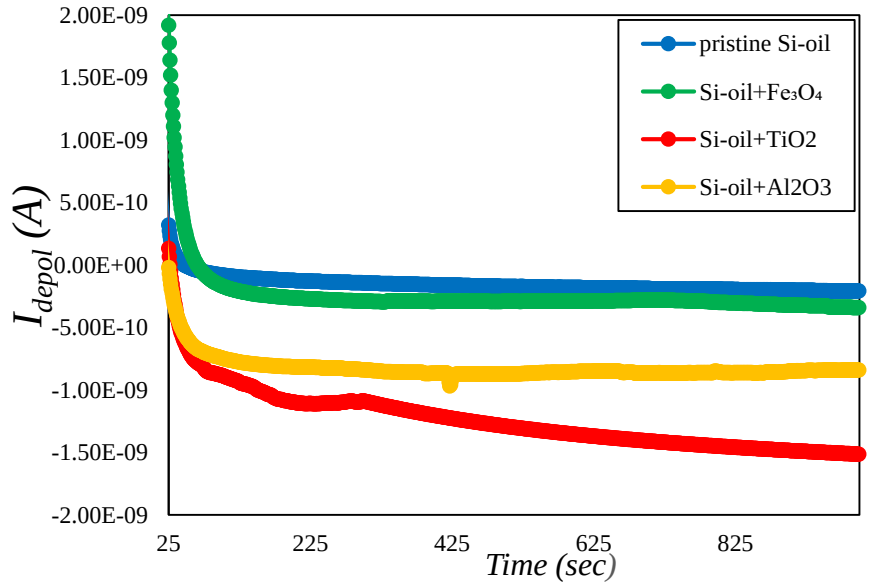

Fig. 15: Variation of Depolarization current of different samples at 30^{0}C

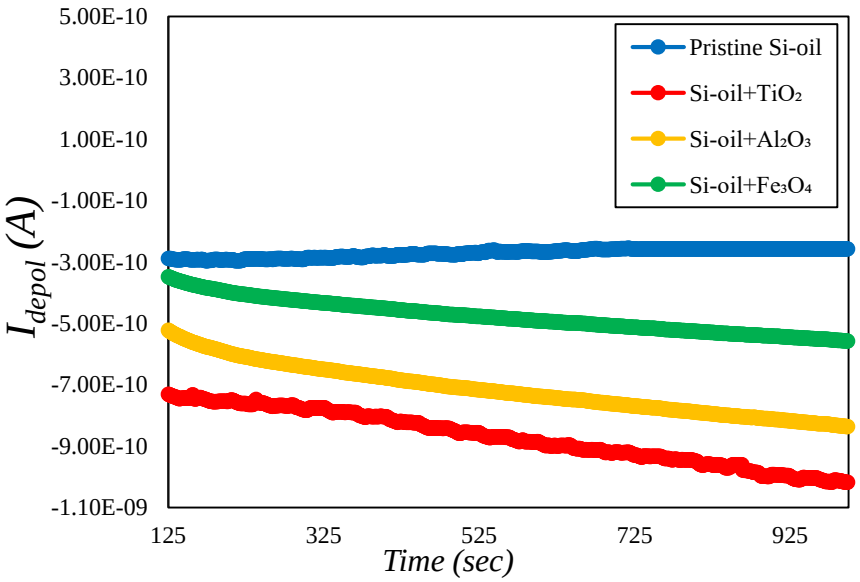

Fig. 16: Variation of depolarization current of different samples at 80^{0}C

5.1.4 Variation of DC conductivity of nanofluids with temperature

In this section the effect of different nanoparticles on the DC conductivity of different prepared silicone oil based samples have been studied at different temperatures. In Fig. 17, σ_{dc} of different prepared silicone oil based samples has been plotted for 30℃, 40℃, 50℃, 60℃, 70℃, 80℃ respectively. In this context, the DC conductivity (σ_{dc}) is obtained by using (3.5). It is clearly seen from the Fig. 17, the conductivity increases with the increment in temperature. This is due to a fact that, at higher temperatures conduction current increases because, at high temperature extra number of free electrons by obtaining high thermal energy enters into the conduction band from valance band. This is the primary cause for the increment of conduction current. From the Fig.17, it can also be observed that, nanofluids have shown lower dc conductivity than pristine silicone oil. This can be defined by a fact that, infusion of NP in the base oil might trapped free electrons which moving towards anode.

When TiO_2 NP was introduced in the silicone oil, the σ_{dc} of Si-oil+ TiO_2 nanofluid sample showed least conductivity among all other nanofluid samples. This is due to a fact that, Ti atoms have a higher affinity towards the hydroxyl ions (OH^-) and makes a bond. Which in turn makes a resistance to the free electrons moving towards anode. As a result, the incremental rate of polarization current of TiO_2 nanofluid sample was least among all of the nanofluid samples for this reason the σ_{dc} of si-oil+TiO_2 was lowest least. As silicone oil-based insulation is mostly used in cable termination, which often suffers from extreme electric field distortion. In addition, during the cold environmental

condition, saviour defects can form inside the silicone oil. As a whole, these factors cause significant deterioration in the cable termination by initiating partial discharge in the insulating oil. Hence, the reduced σ_{dc} can play an imperative role in minimizing the impact of partial discharge by confining discharge propagation. According to the [40] the addition of nanofillers has played a significant role in improving the dc conductivity of silicone oil. So, addition of TiO_2 NP into the silicone oil for reducing dc conductivity is beneficial for higher temperature.

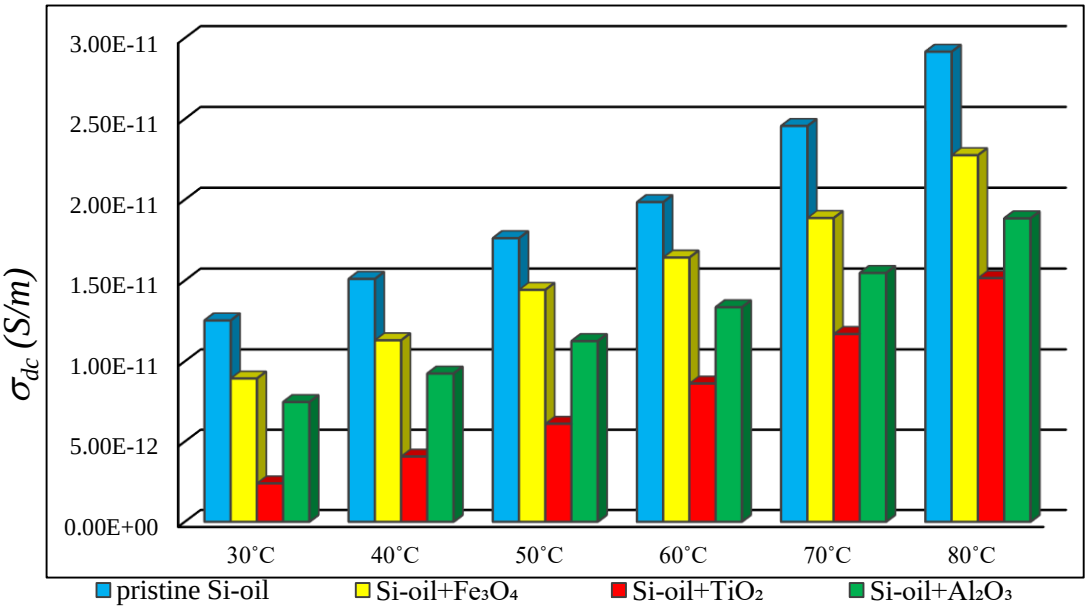

Fig. 17: Variation of σ_{dc} of different samples at different temperatures

5.1.5 Estimation of activation energy (E_g) of nanofluids

In this section the activation energy of different prepared silicone oil-based nanofluid samples have been calculated using equation (3.9). As mobility of charge carriers depends upon temperature effectively, it has a dominating role on polarization process in dielectric medium [34]. It can be revealed that, the change of conductivity with the change in temperature is associated with the activation energy (E_g). The activation energy of the prepared samples is presented in the Table 1. From the Table 1 it can be concluded that Eg of silicone oil based Fe3O4 and Al_2O_3 samples both improved by 13.34% and TiO_2 samples improved by 126.67% over pristine oil. This is due to a fact that, Ti has a strong affinity towards hydroxyl ions (OH^-) and thus titanium might offer strong bonding with hydroxyl ions (OH^-). This bonds may offer a strong resistance for the free electrons moving towards anode. To overcome these resistive barriers electrons

might need more energy, for this reason activation energy of silicone oil based TiO_2 nanofluid was improved.

Table 1: Activation energy (E_g) of different prepared samples

Sample	Activation energy (eV)
Pristine Si-oil	0.15
Si-oil+Fe_3O_4	0.17
Si-oil+TiO_2	0.34
Si-oil+Al_2O_3	0.17

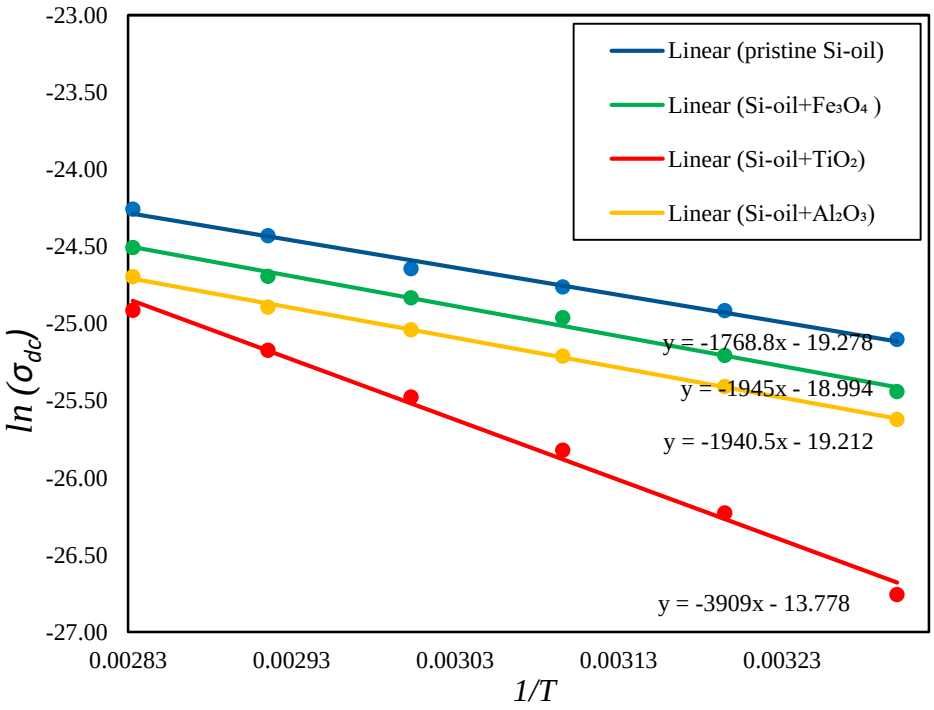

Fig. 18: The fitted curves of $ln(\sigma_{dc})$ vs 1/T of silicone oil based nanofluids

It can be observed from the above calculation that silicone oil based alumina and Fe_3O_4 nanoparticles have less activation energy than TiO_2 contained nanofluid. But all the nanofluids have more activation energy than pristine oil. That refers blending of nanoparticles improve activation energy. So, electrons present in the nanofluids needed more energy to start conduction than electrons present in the pristine silicone oil.

5.2 Dielectric Response in Frequency Domain of Nanofluids

In this section, dielectric response measurements in the frequency domain have been elaborated. Frequency domain responses of pristine silicone oil along with nanofluid samples were analyzed at different temperatures (30℃, 40℃, 50℃, 60℃, 70℃ and

80°C). In the later part, the low frequency dispersion characteristics of ε', ε'', and $tan\delta$ are illustrated.

5.2.1 Variation of Real Component of the Complex Permittivity with Different Nanoparticles

In this section, the effect of different nanoparticles on the real component of the complex permittivity have been studied. In Fig. 19- Fig. 20, showing plots for the real component of complex permittivity *(ε')* for various prepared samples at different temperatures. From Fig. 19 - Fig. 20, it can be observed that, there is a significant variation in the low frequency region of the *(ε')* which is associated with the interfacial polarization. Further, the nanofluid samples have shown a significant decrease in the interfacial polarization, which is attributed by the accumulation of charges at the electrode/oil interface. Hence, it can be deduced that the presence of nanoparticles has a positive impact in suppressing the interfacial charge polarization. As a result, the effect of parasitic capacitance has been substantially curtailed, which is reflected by the decrement in the ε' in the low frequency region of 10^3 Hz -10 Hz.

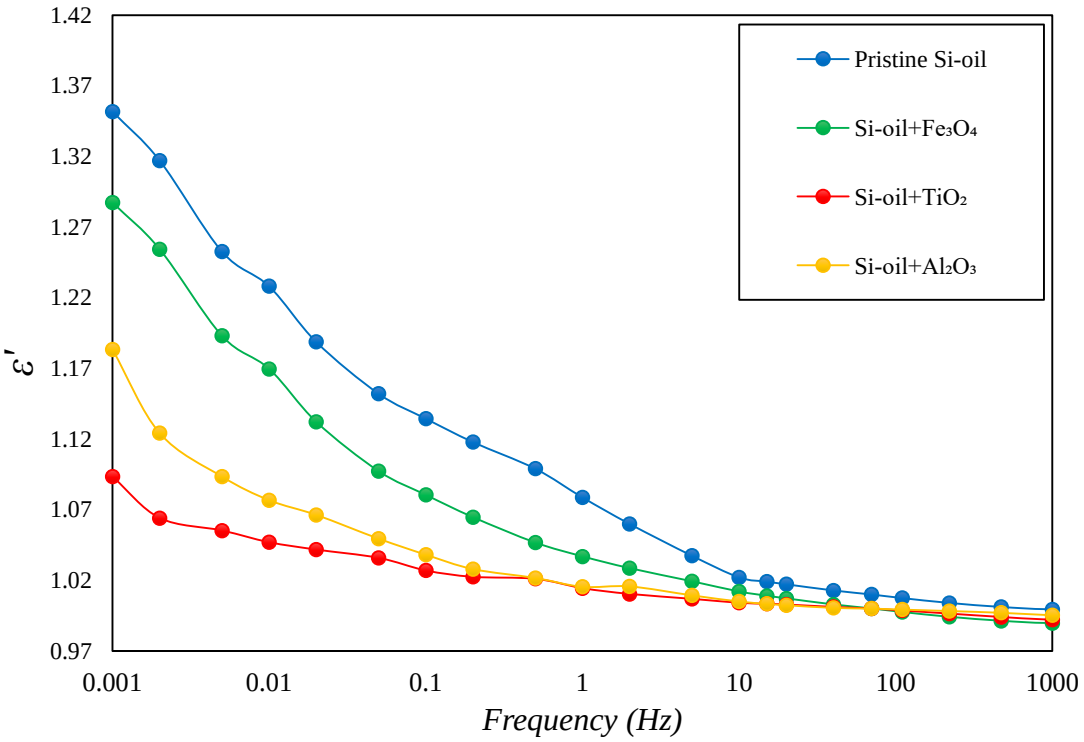

Fig. 19: Variation of ε' of different samples at 30^0C

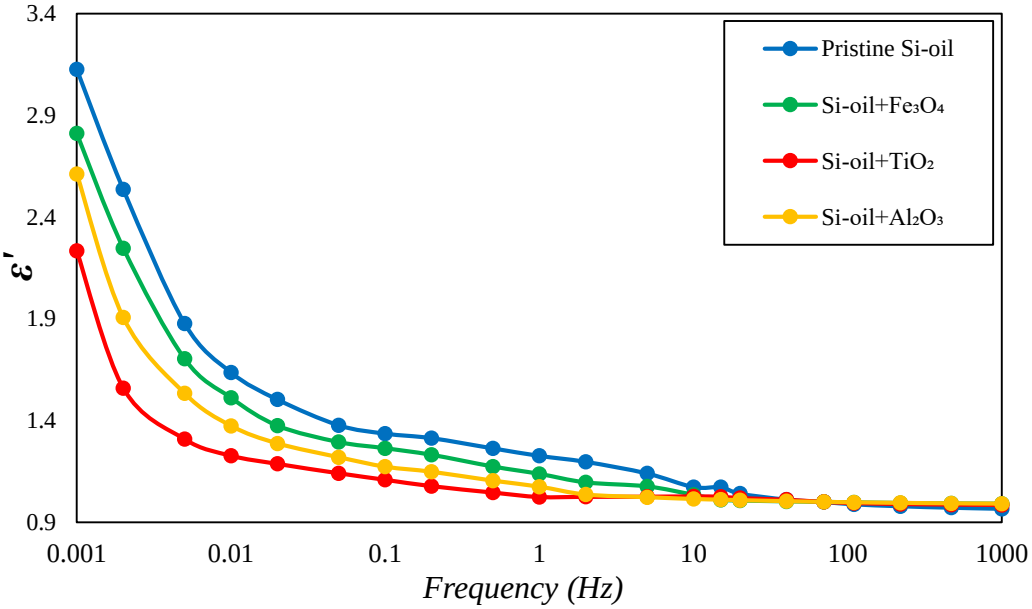

Fig. 20: Variation of ε' of different samples at 80^0C

5.2.2 Variation of Real Component of the Complex Permittivity with temperatures

In this section, the effect of temperature on the real component of the complex permittivity of the prepared nanofluid samples have been studied. In Fig. 21 – 24, the real component of the complex permittivity (ε') of the nanofluids have been plotted against frequency at different temperatures. From the figures it can be observed that, the peak occurred at low frequency region due to space charge polarization and become minimal at high frequency region irrespective of temperatures. It can be also observed that, the increment rate of (ε') is less in lower temperature range of 30°C - 50°C than the incremental rate in the higher temperature range of 60°C – 80°C.

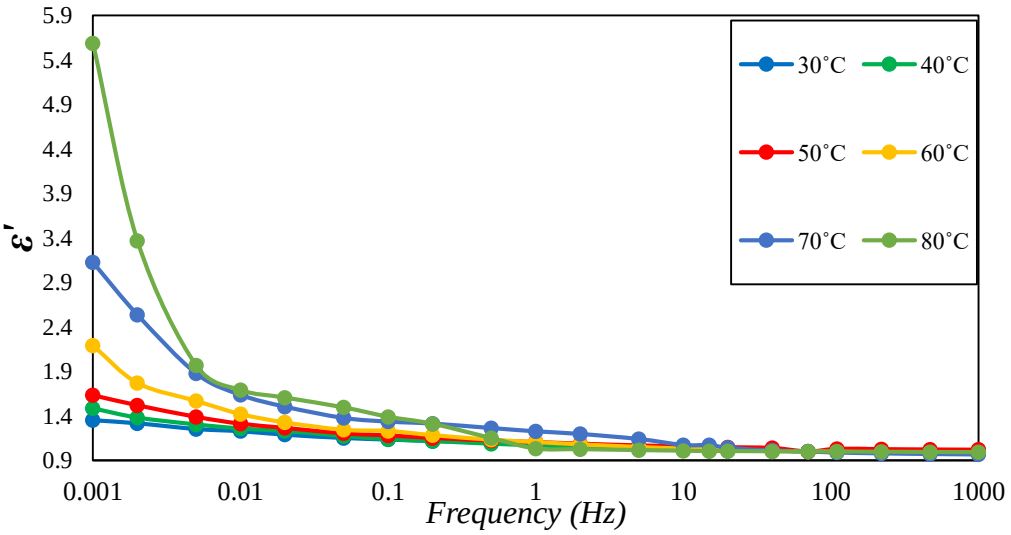

Fig. 21: Variation of ε' of pristine silicone oil at different temperatures

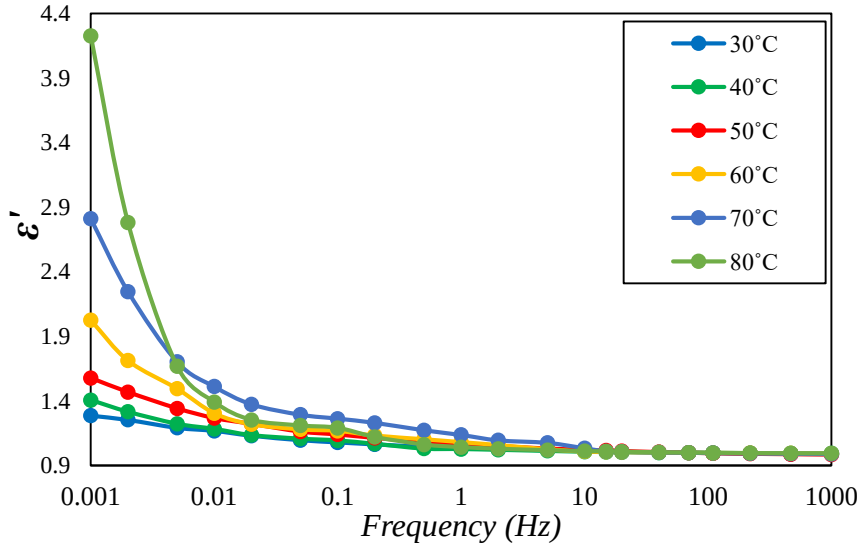

Fig. 22: Variation of ε' of silicone oil based Fe_3O_4 sample at different temperatures

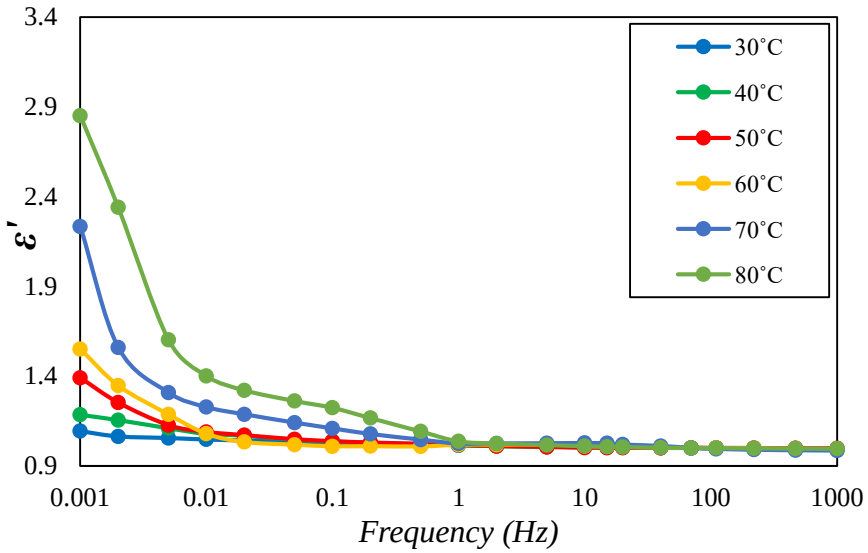

Fig. 23: Variation of ε' of silicone oil based TiO_2 sample at different temperatures

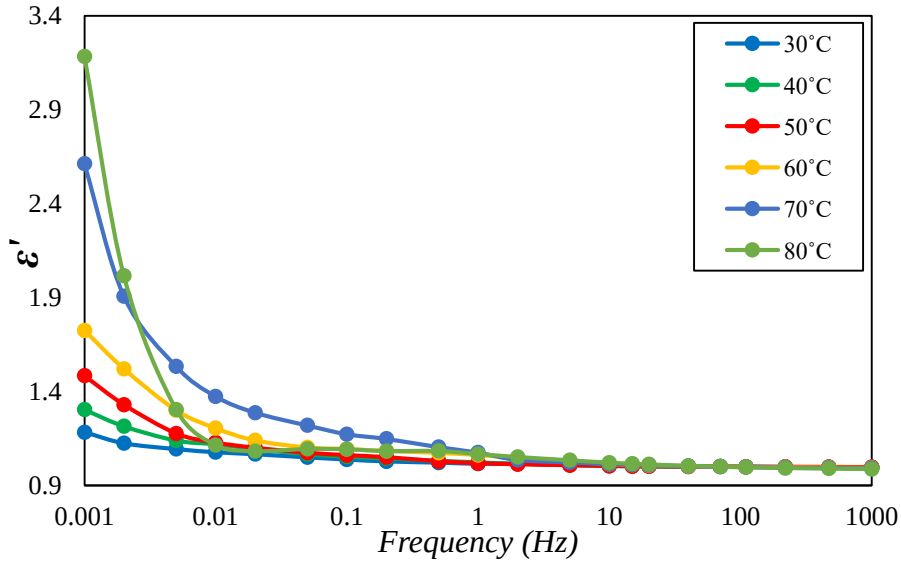

Fig. 24: Variation of ε' of silicone oil based Al_2O_3 sample at different temperatures

This indicates an obvious dependency of ε′ on temperature variation in low frequency region. As discussed in [38], the dielectric constant ε′ is associated with low-frequency polarization at electrode/oil interfacial. Owing to increased temperature, thermal excitation of the charged carriers increases significantly. In addition, the viscosity of the insulating oil decreases. These two factors enable faster polarization of the space charges. Consequently, ε′ steadily increases in lower frequency region.

5.2.3 Variation of imaginary component of the complex permittivity with different nanoparticle

In Fig. 25 - Fig. 26, the impact of nanofiller addition on the dielectric loss factor has been illustrated. It can be observed that with the increase in the temperature the entire spectrum of the ε'' has shown a considerable increment. This phenomenon is mainly driven by several mechanisms such as conduction loss, polarization loss and jump conductance. However, the increase in the temperature causes the mobility of the space charges of the insulation to increase significantly. This results in an elevated conduction loss in the insulating material, which is confirmed by a significant increase in the low frequency segment (10^{-3} Hz – 1 Hz) of the ε'' curve. In this context, the Si-oil+TiO_2 and Si-oil+Al_2O_3 have showed better dielectric performance by restraining the conduction of charges through the restriction of the free mean path in the bulk of the insulation. As a whole, it can be manifested that the combination of suppression of interfacial charge accumulation and reduced conduction loss has been achieved by the TiO_2 and Al_2O_3 nanoparticle addition.

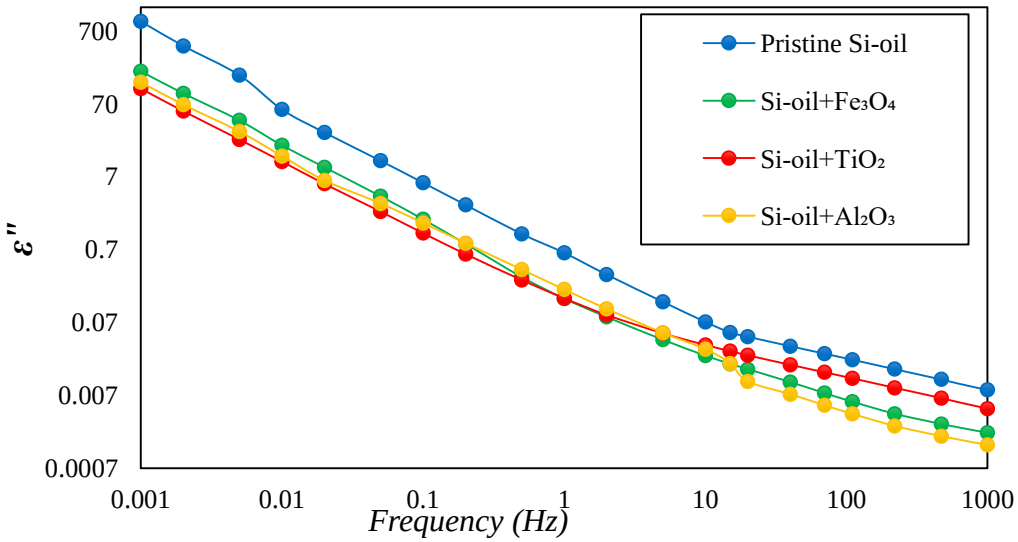

Fig. 25: Variation of $\varepsilon''$of different samples at 30^0C

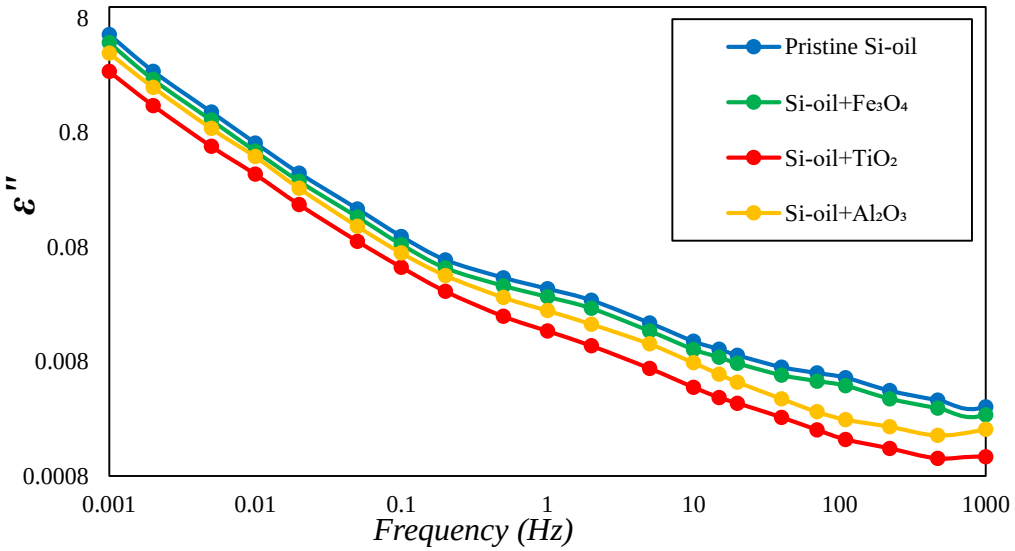

Fig. 26: Variation of $\varepsilon''$of different samples at 80^0C

5.2.4 Variation of imaginary component of the complex permittivity with temperature

In this section, the effect of temperature on the img. component of the complex permittivity of the prepared nanofluid samples have been studied. In Fig. 27- 30, the img. component of the complex permittivity (ε'') of the nanofluids have been plotted against frequency at different temperatures. From the figures it can be observed that, for all of the prepared samples the peak occurred at low frequency region due to space charge polarization and become minimal at high frequency region irrespective of temperatures.

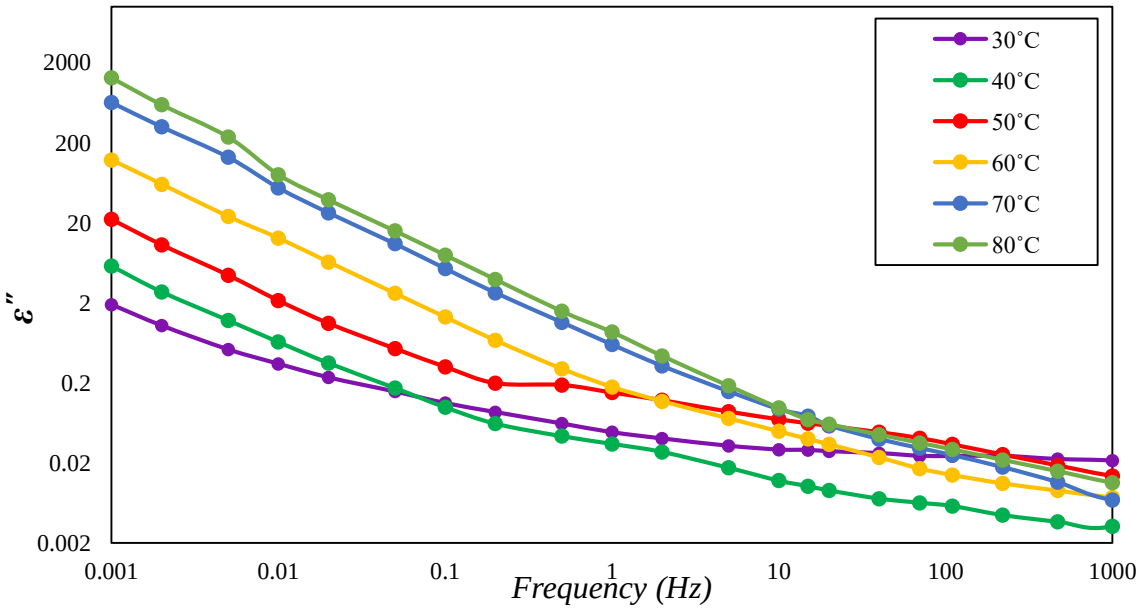

Fig. 27: Variation of $\varepsilon''$of pristine silicone oil samples at different temperatures

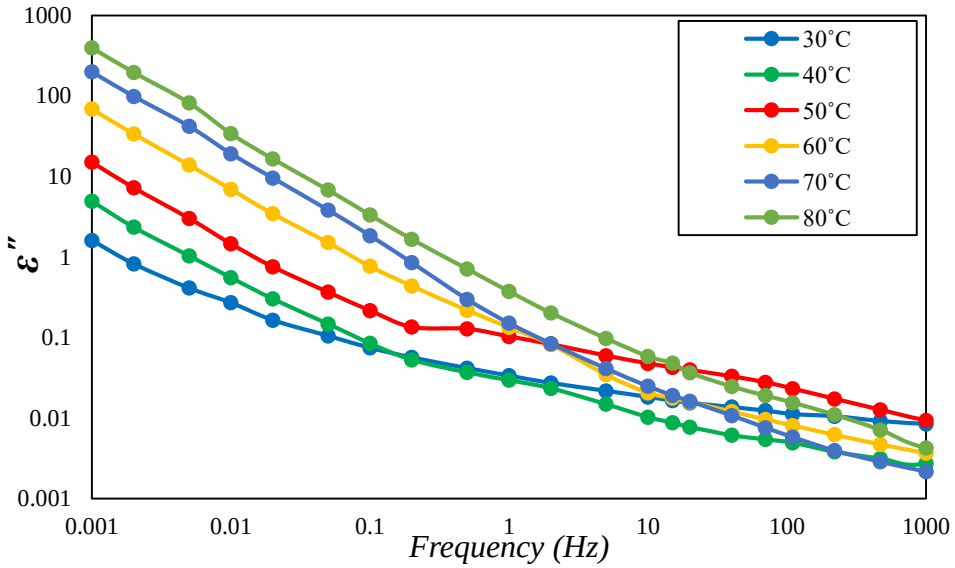

Fig. 28: Variation of $\varepsilon''$of silicone oil based Fe_3O_4 sample at different temperatures

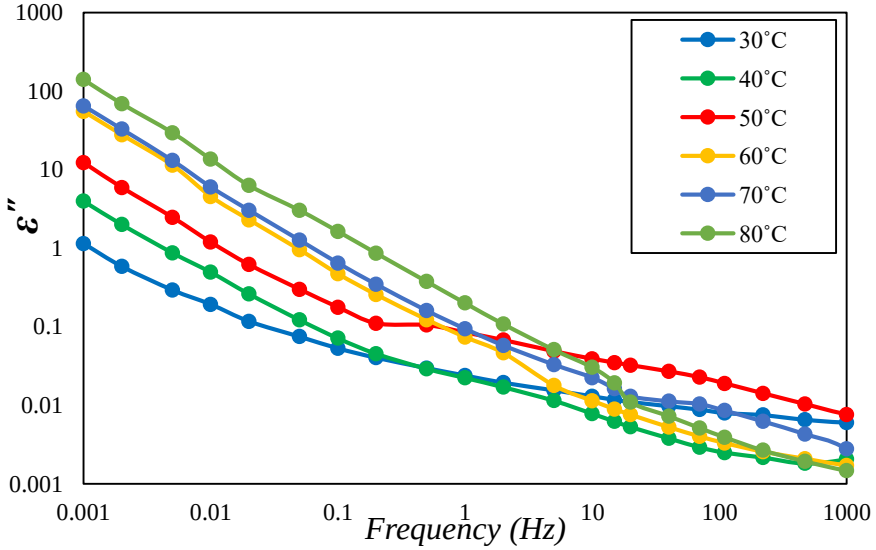

Fig. 29: Variation of $\varepsilon''$of silicone oil based TiO_2 sample at different temperatures

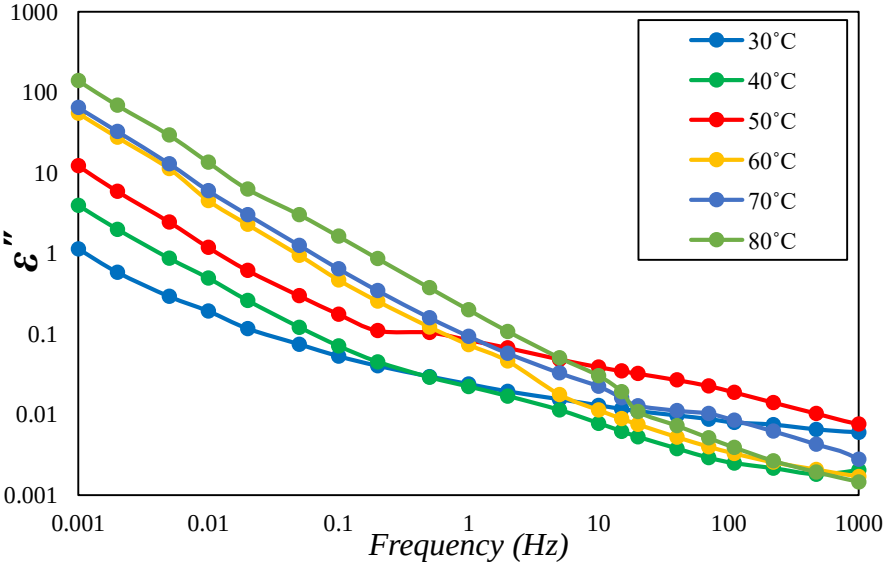

Fig. 30: Variation of $\varepsilon''$of silicone oil based Al_2O_3 sample at different temperatures

5.2.5 Variation of *tanδ* of pristine silicone oil and other three nanofluids with different nanoparticles

In this section, the *tanδ* profiles of different prepared samples have been plotted at different temperatures which are shown in Fig. 32 - Fig. 37. From the figures, it can be observed that the peak in the *tanδ* profile occurs at low frequency region and turns into a minimum at high frequency region. Dipoles are formed at the interfaces between various materials, such as between dielectric and conductor materials, when mobile positively and negatively charged particles are separated under an applied field. *Tanδ* have been calculated by using fds data given from IDAX 300. From Fig. 35 - Fig. 37, it has been observed that, the *tanδ* value of (Si-oil + TiO2) nanofluid is higher than the corresponding value of pure silicone oil at high frequency range. This may be due to the unbalanced crystal structure of TiO_2 nanoparticles. The molecular structure of TiO2 nanoparticles has been shown by Fig. 31. It may be observed from Fig. 31, that the inter atomic distance between one Ti-O atom is nearly 1.988 Å, whereas the distance between another Ti-O bond is around 1.944 Å [32]. This unbalance structure of the TiO2 nanoparticles develop the strong polarization characteristics in the crystal [32]. It is reported in [33] that the relaxation time of polar crystal, specially TiO2 ranges from 10^{-13} to 10^{-3}s. Therefore, the unbalanced structure of TiO2 molecules in crystal takes part in the dipole polarization during FDS near to kHz range. This explains the polarization process at higher frequency range, which causes large interactions due to the polar crystal TiO2 in nanofluids that results in higher value of *tanδ* at higher frequency range.

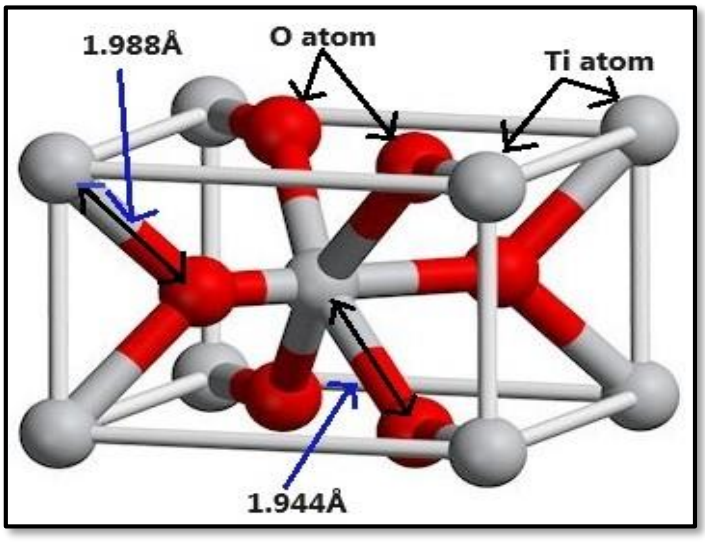

Fig. 31: Typical crystal structure of a TiO_2 nanoparticle [31]

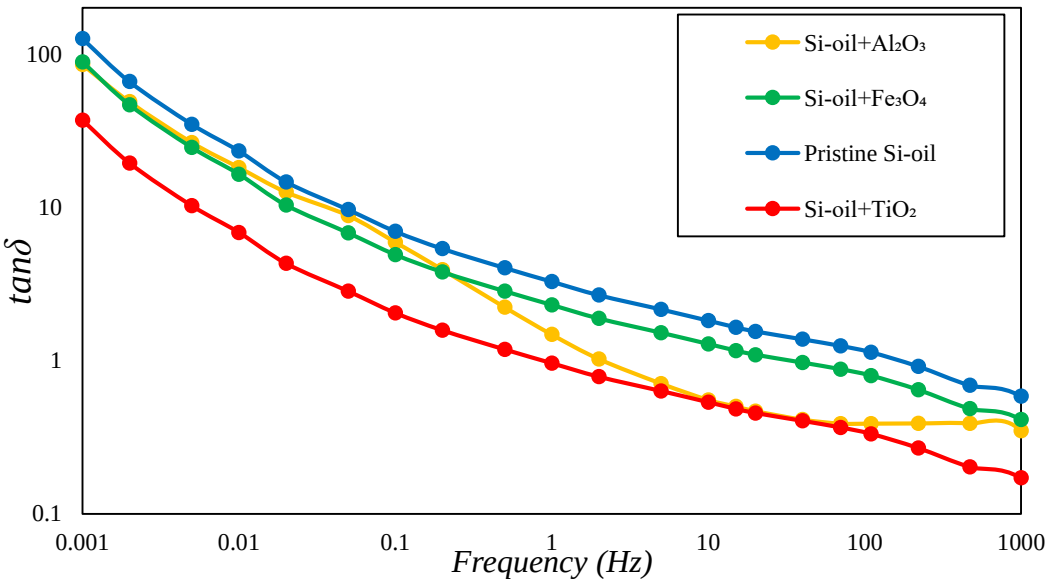

Fig. 32: Variation of *tanδ* of different samples at 30^{0}C

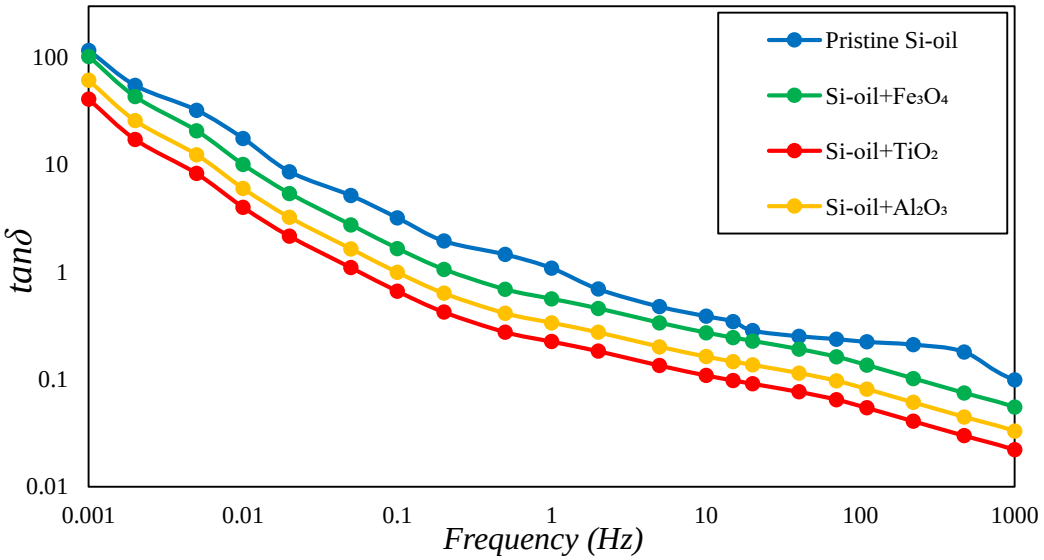

Fig. 33: Variation of *tanδ* of different samples at 40^{0}C

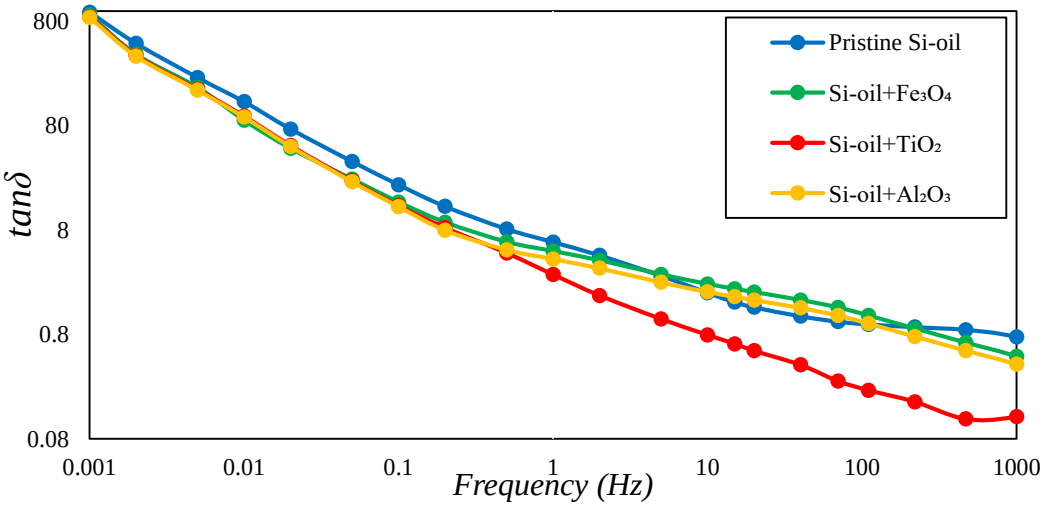

Fig. 34: Variation of *tanδ* of different samples at 50^{0}C

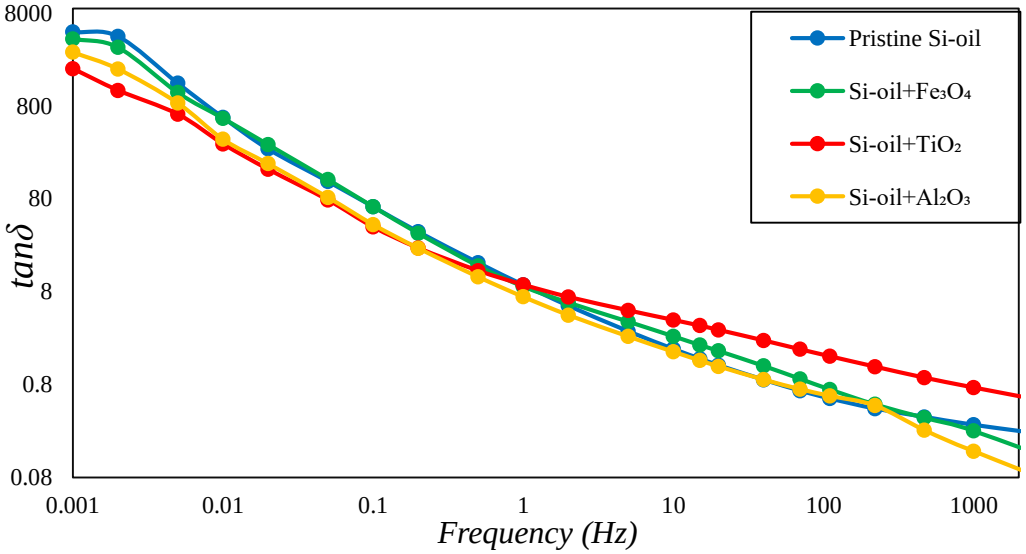

Fig. 35: Variation of *tanδ* of different samples at 60^{0}C

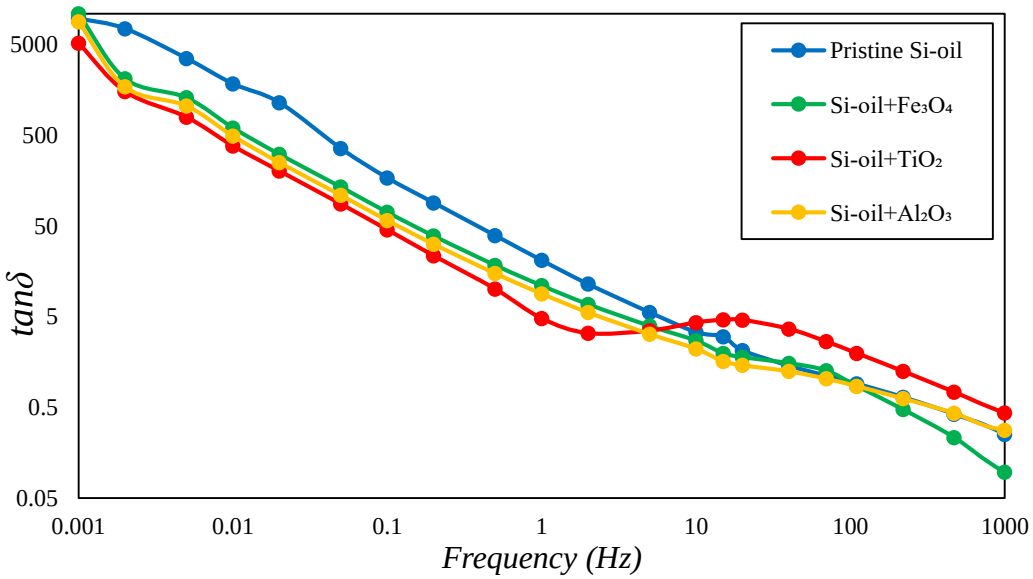

Fig. 36: Variation of *tanδ* of different samples at 70^{0}C

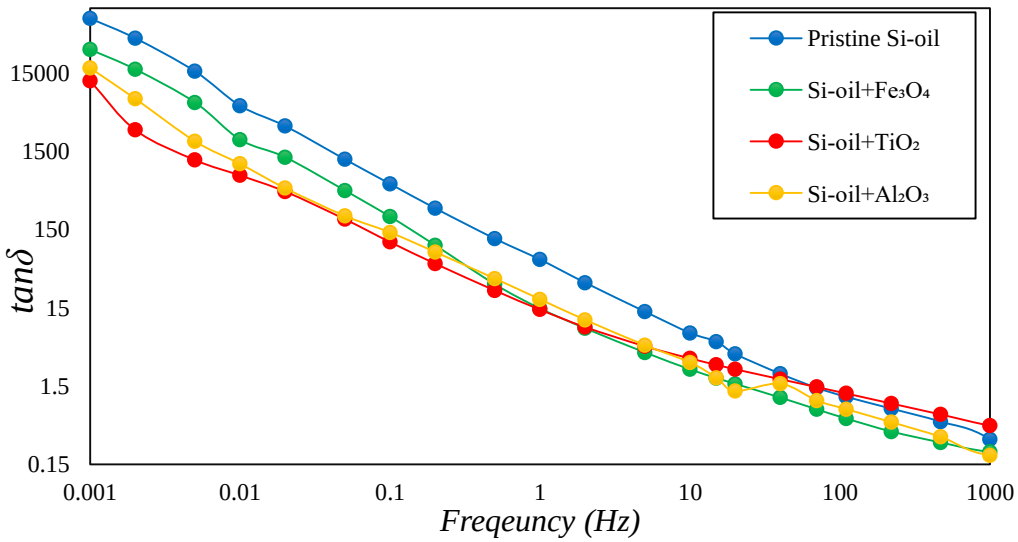

Fig. 37: Variation of *tanδ* of different samples at 80^{0}C

5.2.6 Variation of AC conductivity of nanofluids with different nanoparticles

AC conductivity of the silicone oil based nanofluids can be determined properly by using frequency domain spectroscopy. AC conductivity can be derived from (5.1).

$$\sigma = \frac{C'' \times \varepsilon_0 \omega}{C_0} \tag{5.1}$$

Where, σ is the ac conductivity, C″ is imaginary capacitance, ε_0 is permittivity in free space (8.854×10^{-12} F/m) and C_0 is geometrical capacitance of the aluminium electrode. Therefore, the ac conductivity of different prepared samples has been plotted at different temperatures as shown in Fig. 38 - Fig. 39. From plotted figures it can be observed that the value of the σ_{ac} is lowest in low frequency region for all the samples and gradually increases with frequency as σ_{ac} is a function of ω according to equation (5.1). It can be observed that the value of ac conductivity for all the nanofluids is less than pristine silicone oil irrespective for all the temperatures. Silicone oil based TiO_2 nanofluid has the lowest value of ac conductivity. It can be claimed that, σ_{ac} is deduced due to injection of nanoparticle in the insulating oil. As σ_{ac} is purely depending on C'', considering other parameters are constant. C'' is directly proportional to ε'' and it has been already discussed in 5.2.3 that, ε'' of nanofluid samples is less than pristine silicone oil irrespective of temperature. Therefore, prepared nanofluid samples have been showing less σ_{ac} than pure silicone oil.

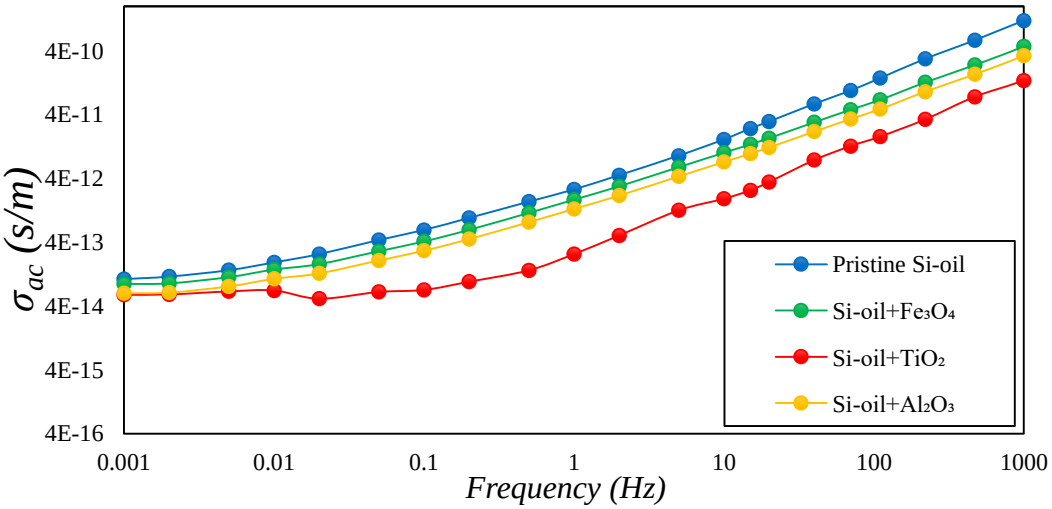

Fig. 38: Variation of σ_{ac} of different samples at 30^0C

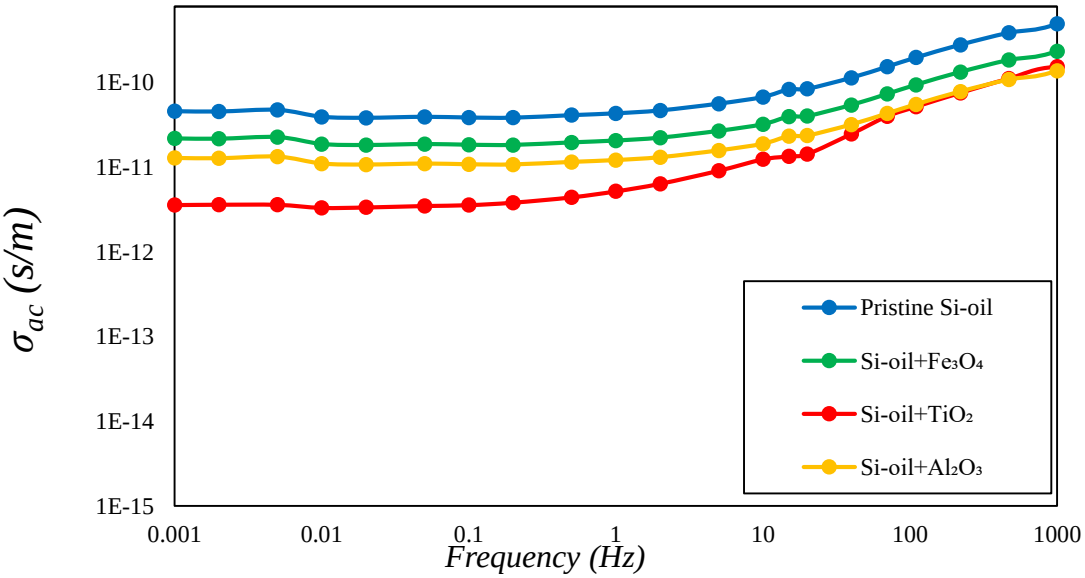

Fig. 39: Variation of σ_{ac} of different samples at 80^{0}C

5.2.7 Variation of AC conductivity of nanofluids with temperature

In this section, the effect of temperature on the ac conductivity (σ_{ac}) of the prepared nanofluid samples have been studied. In Fig.40 - the ac conductivity (σ_{ac}) of the nanofluids have been plotted against frequency for different temperatures. From the figures it can be observed that, for all of the prepared samples the peak occurred at high frequency region and become minimal at low frequency region irrespective of temperatures. It can be observed that samples with nanoparticles injected have shown less conductivity than pristine silicone oil in low frequency region irrespective of temperature.

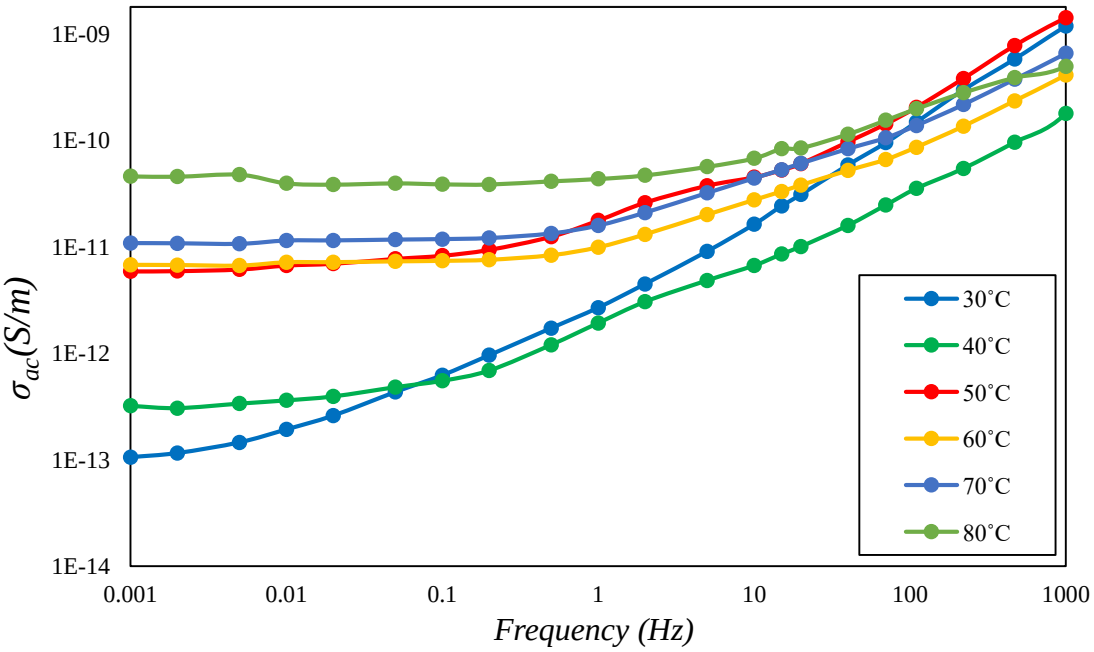

Fig. 40: Variation of σ_{ac} of pristine silicone oil samples at different temperature

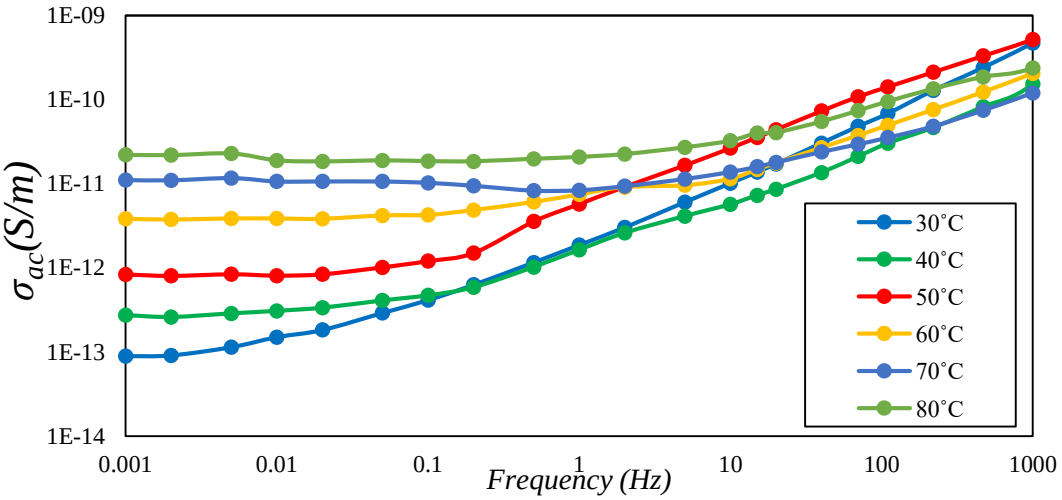

Fig. 41: Variation of σ_{ac} of silicone oil based Fe_30_4 sample at different temperatures

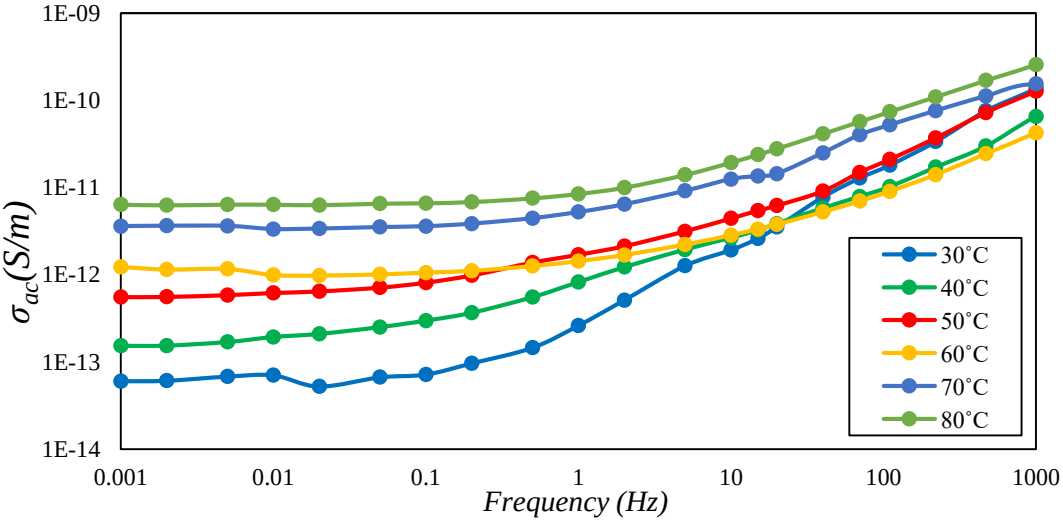

Fig. 42: Variation of σ_{ac} of silicone oil based TiO_2 samples at different temperatures

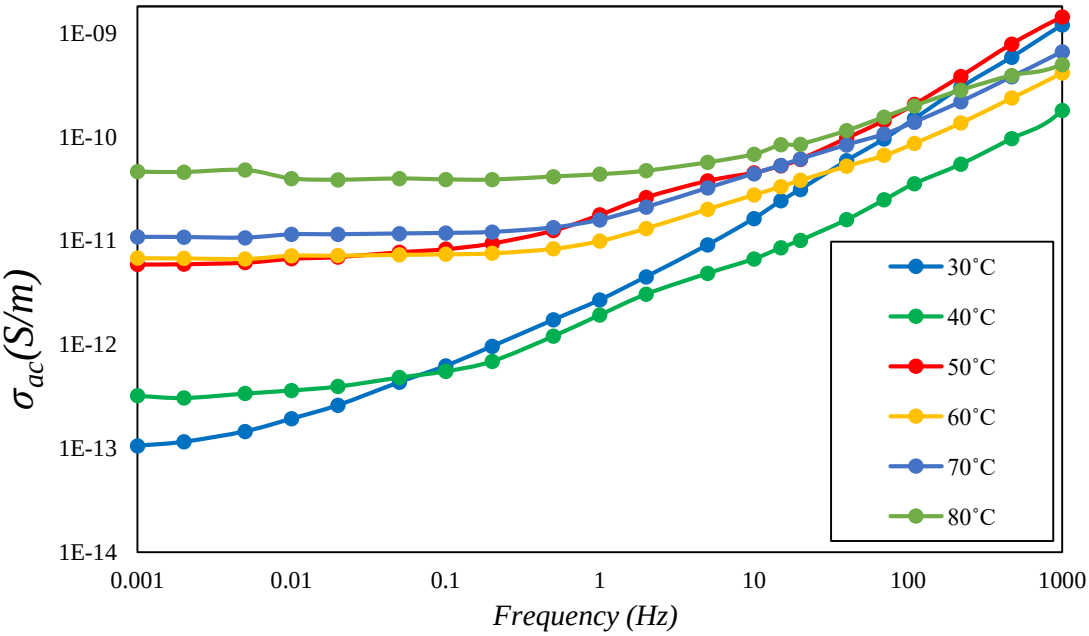

Fig. 43: Variation of σ_{ac} of silicone oil based Al_2O_3 samples at different temperatures

5.2.8 Variation of Electric Modulus of nanofluids with different nanoparticles

In Fig. 44 – Fig. 49 the electric modulus of different prepared nanofluid samples has been plotted with varying temperatures using (3.19). From Fig. 45.- Fig. 49, it can be elucidated that, the peaks of electric modulus of nanofluid samples have been observed to be in the low frequency region (10^{-3} Hz- 10^{0} Hz) within the temperature range of 30^{0} C to 60^{0} C. It can be clearly seen from the fig that, in the low frequency region $M"(\omega)$ is significantly increasing and after reached to a peak value decreased again in the higher frequency range and formed a bell-shaped curve. It is due a fact that, in the dispersion region the imaginary part of the complex permittivity $\varepsilon''(\omega)$ decreases faster than the real part of the complex permittivity $\varepsilon'(\omega)$ with increment in frequency [41]. This dielectric loss due to electrode polarization had been greatly reduced. Therefore, a distinct peak corresponding to each figure of $M"(\omega)$ curves which was related to the relaxation behavior of the dielectric oil. The value of frequency related to each distinct peak is defined as the peak-frequency (f_p). The effect of the temperature on the peak frequency is to shift the entire $M"(\omega)$ response towards right along the frequency. In view of this depiction, it can be clearly stated that, the incorporation of TiO_2 has shown the most improved dielectric characteristics by constraining the polarization phenomenon even at elevated temperature.

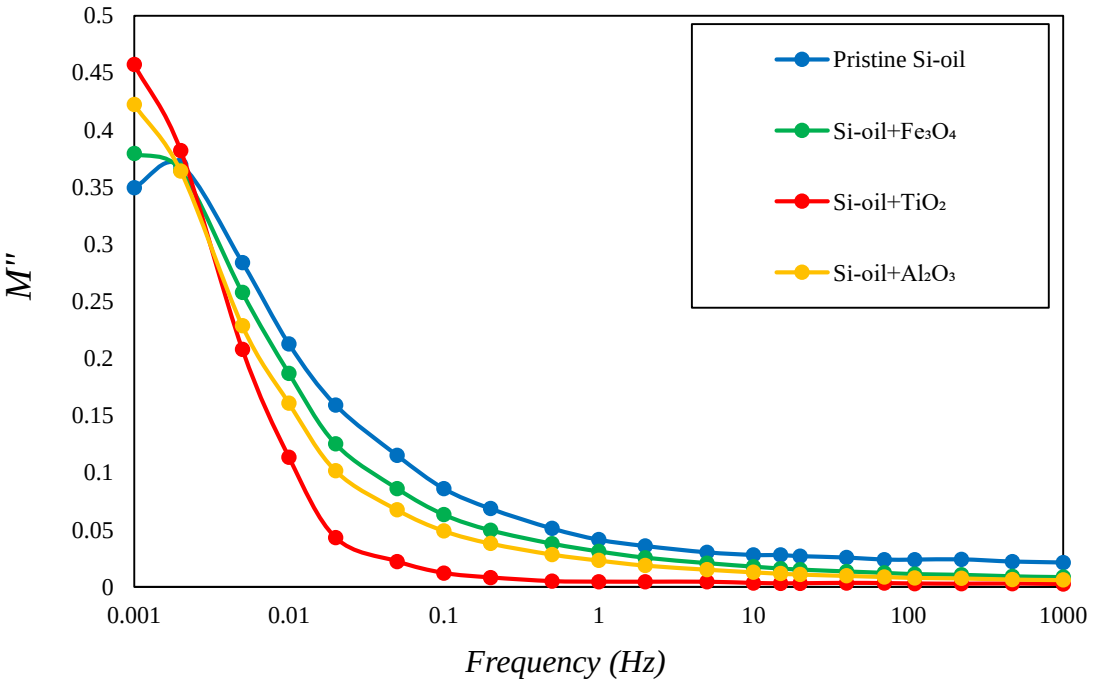

Fig. 44: Variation of M'' of different samples at 30^{0}C

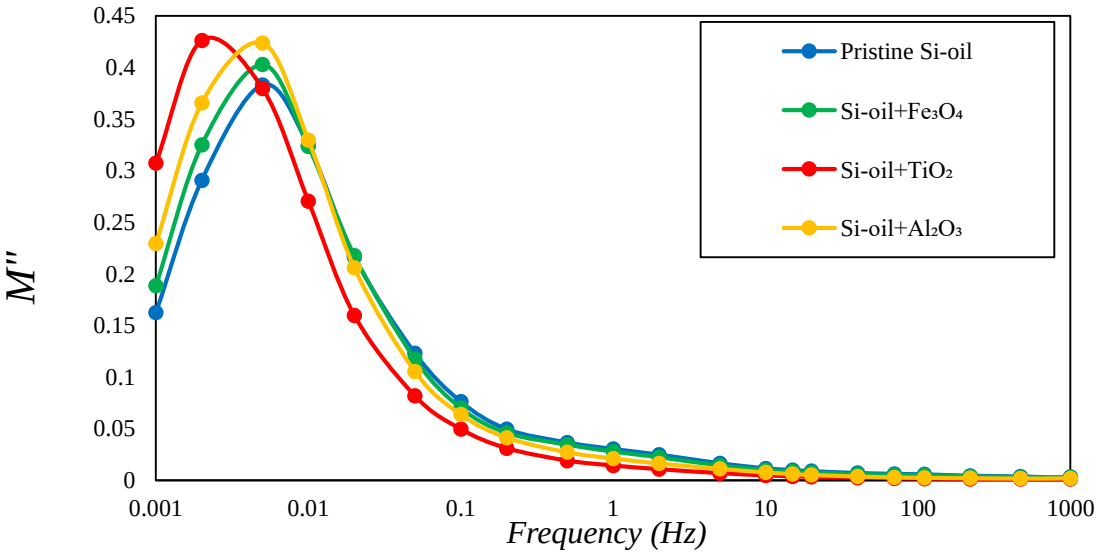

Fig. 45: Variation of M'' of different samples at 40^0C

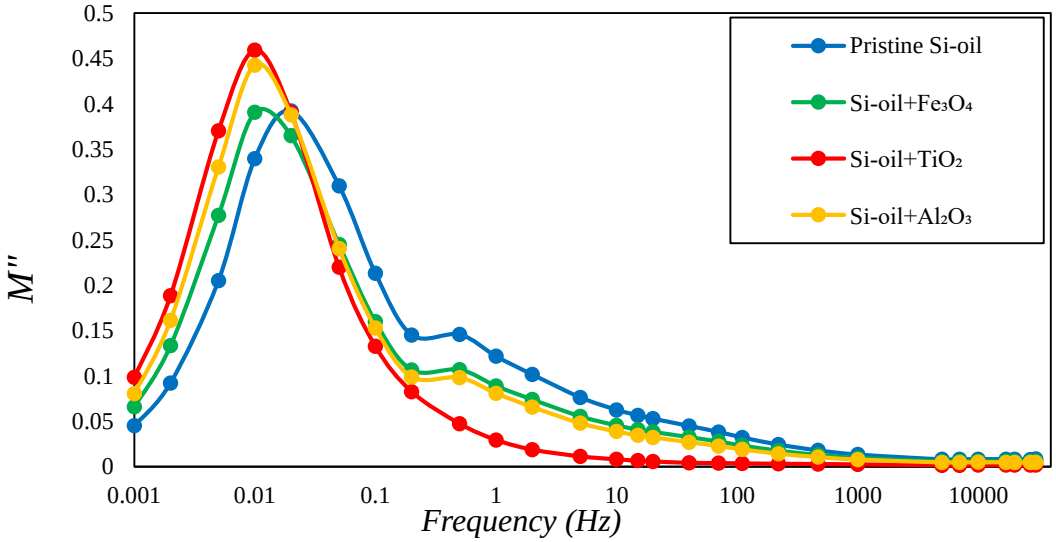

Fig. 46: Variation of M'' of different samples at 50^0C

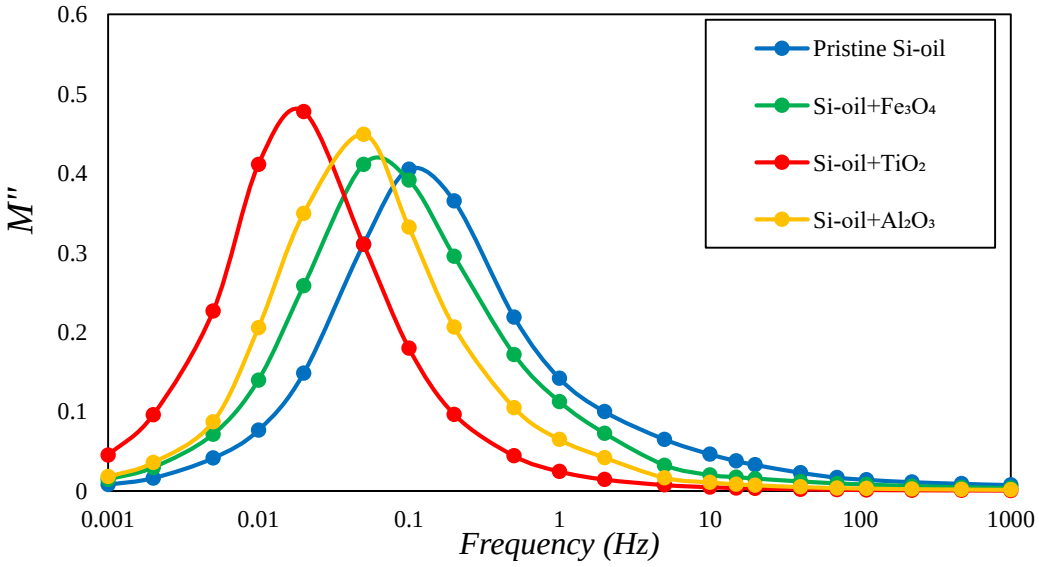

Fig. 47: Variation of M'' of different samples at 60^0C

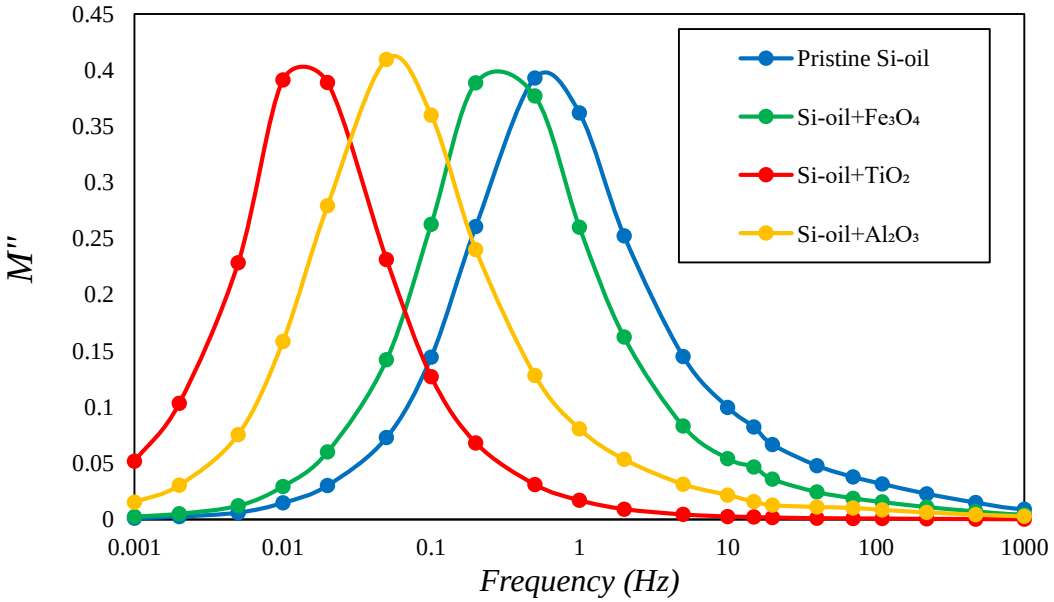

Fig. 48: Variation of M'' of different samples at 70^0C

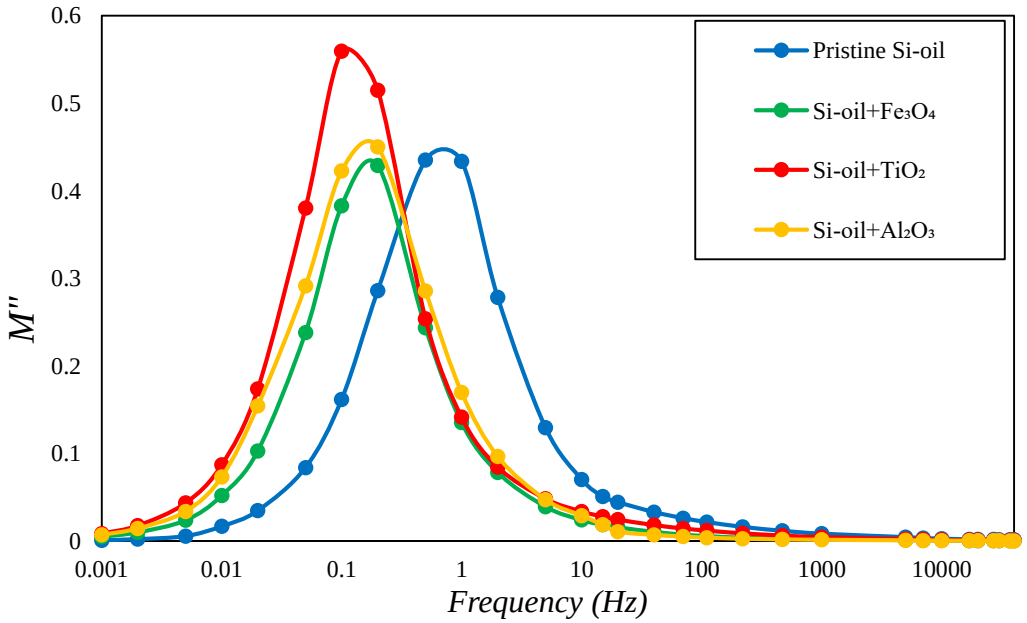

Fig. 49: Variation of M'' of different samples at 80^0C

5.3 Breakdown voltage measurement

The results of power frequency AC breakdown strength (BDS) tests of different silicon oil based nanofluid samples along with pristine sample have been shown in Fig. 50. From the Fig. 50, it can be observed that the incorporation of TiO_2 and Al_2O_3 nanoparticle enhances the breakdown strength of the silicone oil insulation by 17.78% and 12.58% respectively. However, Fe_3O_4 nanoparticle has shown a negative impact on the BDS of the insulation sample, since, owing to its conductive property, Fe_3O_4 nanoparticle incorporation has caused a reduction in BDS by 13.8% compared to pristine silicone oil.

It is due to a well- known fact that hydroxyl ions have an affinity towards Ti atoms. As a result, they attached on the surface of the Ti atoms and behaved as a negatively charged particles [28]. In the presence of an electric field a bond has been developed in between Ti atom and Hydroxyl ion (OH^-). In case of Al_2O_3 based nanofluids, hydrogen ions (H^+) have an affinity towards O atoms present in the alumina and, thus behave as a negatively charged particles. These negatively charged particles migrate slower than the electrons, minimizing the propagation velocity of ion in the base oil by scavenging them. As a result of this phenomenon, a resistance has been developed against streamer propagation of free electrons present in the sample. These bonds are capable of trapping free electrons present in the sample and possibility of streamer propagation has been decreased [28]. It may be concluded that, the streamer development is one of the most expected causes of the breakdown voltage in insulating oils. The electron avalanche process is primarily responsible for this streamer formation. Therefore, the number of free charges plays a crucial role in the electron avalanche phenomena. So, the primary cause of the breakdown voltage can be recognized.

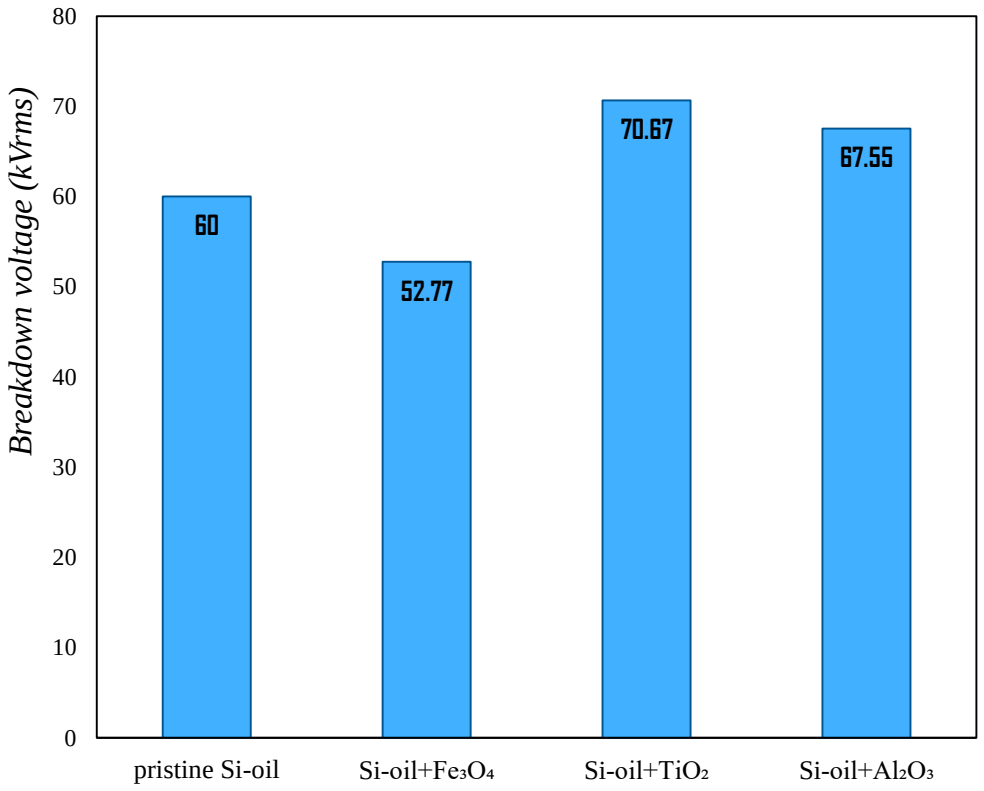

Fig. 50: AC BDV of silicone oil nanofluids

CHAPTER 6

CONCLUSIONS

6.1 Conclusions

In this work, it has been examined that inducing different nanoparticles into the liquid insulation is beneficial to improve the dielectric properties of insulating oil dielectric spectroscopic methods. For these purposes, dielectric spectroscopic measurements have been conducted in both the time and the frequency domains. From these measurements, several parameters have been extracted with variation of temperatures with constant percentage concentrations of nanoparticles in the laboratory prepared silicone oil based nanofluids. It can be concluded that, form the calculated parameters, silicone oil base TiO_2 and Al_2O_3 nanofluids showed better dielectric performance than pure silicone oil and TiO_2 nanofluid have been shown highest AC breakdown voltage among all the sample.

6.2 Future Scope

Future works can be directed in other different directions. Some of the possible works are mentioned below.

1. This work mainly examined the electrical properties of silicone oil based prepared nanofluid samples. In future, thermal properties of the nanofluids will be studied.
2. In future plan, it will be tried to investigate the electrical properties of silicone oil based hybrid nanofluid by combining two or more than two nanoparticles induced in the silicone oil.
3. In future, it will be tried to investigate about stability of these nanofluids.
4. This work is about the electrical properties of the silicone oil based nanofluids, in near future, it will be tried to investigate the ageing of these silicone oil based nanofluids.

REFERENCES

[1] Method for Determination of Electric Strength of Insulating Oils, Indian Standard 6792, 1992.

[2] https://www.elandcables.com/the-cable-lab/faqs/faq-what-are-the-main-causes-of-electrical-cable-failure

[3] P. Streit, K. Gallego, and F. Gahungu, "Dry terminations for high voltage cable system," in Proc. Int. Conf. Insulated Power Cables, 2011, pp. 1–5.

[4] Q. B. Lai *et. al.,* "Investigation of tail pipe breakdown incident for 110 kV cable termination and proposal of fault prevention," Eng. Fail. Ana., vol. 108, Jan. 2020, Art. no. 104353.

[5] C. AJ *et. al.,* ''Causes of transformer failures and diagnostic methods—A review,'' Renew. Sustain. Energy Rev., vol. 82, pp. 1442–1456,2018.

[6] M. I. Hasan, ''Improving the cooling performance of electrical distribution transformer using transformer oil—Based MEPCM suspension,'' Eng. Sci.Technol. Int. J., vol. 20, no. 2, pp. 502–510, 2017.

[7] M. J. Heathcote, ''Electric power transformer engineering, third edition [book reviews],'' IEEE Power Energy Mag., vol. 11, no. 5, pp. 94–95,2013.

[8] M.H. Ahmadi *et.al.,* "A review of thermal conductivity of various nanofluids," Journal of Molecular Liquids, vol.265, no.3, pp.181–188, 2018.

[9] J. Li *et. al.,* "Solidification Dynamics of Silicone Oil and Electric Field Distribution Within Outdoor Cable Terminations Subjected to Cold Environments," in IEEE Transactions on Power Delivery, vol. 37, no. 5, pp. 4126-4134, Oct. 2022.

[10] Wang, X. *et. al.*, "Review of research progress on the electrical properties and modification of mineral insulating oils used in power transformers," Energies, vol.11, no.3, pp. 487,2018.

[11] S. Thakur *et. al.,* "A comparative analysis of different dielectric fluids for cable sealing ends," 2020 IEEE 3rd International Conference on Dielectrics (ICD), Valencia, Spain, 2020, pp. 762-765.

[12] W.S. Zaengl, “Dielectric spectroscopy in time and frequency domain for HV power equipment. I. Theoretical considerations,” IEEE Electr. Insul. Mag., vol.19, no.5, pp.5–19,2003.

[13] A. Ghaderi *et.al.,* “Effects of temperature on MV cable joints tan delta measurements,” in Proceedings of IEEE Transactions on Dielectrics Instrument Measurement, vol.68, no.10, pp.3892–3898, 2019.

[14] A.K. Pradhan *et.al*., “Determination of optimized slope of triangular excitation for condition assessment of oil-paper insulation by frequency domain spectroscopy,” in Proceedings of IEEE Transaction on Dielectrics Electrical Insulation, vol.23, no.3, pp.1303–1312, 2016.

[15] https://galathermo.com/blog/index.php/2019/02/05/basics-of-cable-joints

[16] Choi *et.al.,* “Preparation and heat transfer properties of nanoparticle-in- transformer oil dispersions as advanced energy-efficient coolants,” Curr. Appl. Phys., vol. 8, no.6, pp. 710–712, 2008.

[17] J. Zhang *et. al.,* “Sonochemical formation of single-crystalline gold nanobelts,” Angew. Chem. Int. Ed., vol. 45, no.7, pp. 1116 – 1119 ,2006.

[18] R. Liu *et.al.,* “Fundamental research on the application of nano dielectrics to transformers,” in Proceedings of Annual Report Conf. on Electrical Insulation and Dielectric Phenomena, pp. 423 – 427, Cancun, Mexico, 2011.

[19] P.P.C. Sartoratto *et.al.*, “Preparation and electrical properties of oil-based magnetic fluids,” J. Appl. Phys., vol.97, no.10, pp-917,2009.

[20] M. Chiesa, S.K. Das, “Experimental investigation of the dielectric and cooling performance of colloidal suspensions in insulating media,” Colloids Surf. A, Physicochem. Eng. Aspects, vol.335, pp. 88 – 97,2009.

[21] B. Du *et.al.* “Thermal conductivity and dielectric characteristics of transformer oil filled with BN and Fe_3 O_4 nanoparticles,” in Proc.IEEE Trans. Dielectr. Electr. Insul., vol.22, no.5, pp. 2530 – 2536, 2015.

[22] F. Wang *et.al.*, “Influence of monodisperse Fe_3O_4 nanoparticle size on electrical properties of vegetable oil-based nanofluids,” J. Nanometer., vol. 2015, pp. 3, 2015.

[23] Y. Lv *et. al.*, “Effect of nanoparticle morphology on pre-breakdown and breakdown properties of insulating oil-based nanofluids,” Nanomaterials, vol. 8, no.7 pp. 476, 2018.

[24] S. Thakur *et. al.,* "A comparative analysis of different dielectric fluids for cable sealing ends," 2020 IEEE 3rd International Conference on Dielectrics (ICD), Valencia, Spain, 2020.

[25] Yin, Hong. (2017). Sealing cap for end of electric cable or optical cable and manufacturing method of sealing cap.

[26] Recent Trends in the Condition Monitoring of Transformers 2013 ISBN: 978-1-4471-5549-2

[27] S. Maur *et.al.,* “Investigation on Effects of Thermal Ageing on LDPE Based on Polarization and Depolarization Currents”, in Proc.IEEE International Conference for Convergence in Engineering, pp. 200-204, 2020.

[28] B. Chakraborty *et.al.,* "Insight the Impact of TiO2 and Al2O3 Nanoparticles in Mineral, Vegetable Oil Based on AC Dielectric Properties—Conformity with Weibull Distribution," in IEEE Transactions on Plasma Science, vol. 51, no. 10, pp. 3095-3102, Oct. 2023.

[29] S. Maur *et.al.,* "Sensing the Thermal Aging of Epoxy Alumina Nano-Composites Using Electric Modulus," in IEEE Sensors Journal, vol. 21, no. 10, pp. 12236-12244, May15, 2021.

[30] B. Chakraborty *et.al.,* Investigations on dielectric characteristics of hybrid nanofluids through time and frequency domain spectroscopic measurement,” J. Mol. Liquids, vol. 366, Nov. 2022, Art. no. 120347.

[31] https://www.chm.bris.ac.uk/motm/TiO2/tio2h.htm

[32] B. Chakraborty, *et.al,* Investigation of Dielectric Properties of TiO2 and Al2O3 nanofluids by Frequency Domain Spectroscopy at Different Temperatures, Journal of Molecular Liquids, Volume 330,2021,115642, ISSN 0167-7322.

[33] P. Sun, *et.al,* "Failure of nano-modified oil impregnated paper under repeated impulse voltage: Effects of TiO2 nanoparticles on space charge characteristics," in IEEE Transactions on Dielectrics and Electrical Insulation, vol. 25, no. 6, pp. 2103-2111, Dec. 2018.

[34] I. Fofana, H. Hemmatjou and F. Meghnefi, “Effect of Thermal Transient on the Polarization and Depolarization Current Measurements of Oil-Paper Insulation”, IEEE Trans. Dielectr. Electr. Insul., Vol. 18, No. 2, pp. 513-520, 2011.

[35] Z. Xiang, P. Ding, F. Ma, H. Ni, C. He and J. Deng, "Comparative Study on Dielectric Performance of Thermal Aged Silicone Oil and Mineral Oil," 2020 IEEE International Conference on High Voltage Engineering and Application (ICHVE), Beijing, China, 2020, pp. 1-4.

[36] B. Chakraborty, A. Mondal, *et.al.* "Investigation on Activation Energy and Temperature Conductivity Dependency of Laboratory prepared Mixed Insulation Samples," 2020 IEEE 1st International Conference for Convergence in Engineering (ICCE), Kolkata, India, 2020, pp. 205-209.

[37] Chen, Zhiyong & Tang, Jie & Luo, Chuanxian & Zhang, Jing. (2015). A Study on Aging Characteristics of Silicone Oil in HV Oil-filled Cable Termination Based on Infrared Thermal Imaging Test. MATEC Web of Conferences. 22. 05026. 10.1051/matecconf/20152205026.

[38] B. Chakraborty, A. K. Pradhan, *et.al,* "Study of Nonlinearity, Activation Energy, and Temperature Effect on Al2O3 and TiO2 Nanoparticle-Based Mixed Oil Characteristics by Dielectric Spectroscopy," in IEEE Transactions on Dielectrics and Electrical Insulation, vol. 30, no. 3, pp. 997-1004, June 2023.

[39] https://www.mdpi.com/2076-3417/8/4/587

[40] Biswajit Chakraborty, *et.al.*, Investigations on dielectric characteristics of hybrid nanofluids through time and frequency domain spectroscopic measurement, Journal of Molecular Liquids, Volume 366, 2022.

[41] J. Hao, Y. Xie and N. Taylor, "Frequency-Domain Spectroscopy of Oil and Oil-Impregnated Pressboard with DC Bias," in IEEE Transactions on Dielectrics and Electrical Insulation, vol. 29, no. 2, pp. 370-377, April 2022.